Accumulating evidence suggests that multiple sequential genetic alterations in a cell lineage at the nucleotide and chromosome levels underlie the carcinogenesis of solid tumors. Amplification of chromosomal DNA is one mechanism of activating genes whose overexpression contributes to the development and progression of cancer. Regions of chromosomal amplification in cancer cells frequently harbor oncogenes, such as *MYC* (Little et al., 1983) and *ERBB2* (Di Fiore et al., 1987). Using comparative genomic hybridization (CGH), we have detected novel regions of amplification in a variety of cancer types, including HCC, and we have identified a number of candidate oncogenes from amplicons (Yasui et al., 2001; Yasui et al., 2002; Yokoi et al., 2002; Okamoto et al., 2003; Yokoi et al., 2003). CGH was initially used for genome-wide detection of copy number changes occurring in cancers (Kallioniemi et al., 1992). However, its resolution is limited (5–10 Mb) because it detects segmental copy number changes on metaphase chromosomes.

The recent introduction of high-density oligonucleotide microarrays designed for typing of single nucleotide polymorphisms (SNPs) facilitates high-resolution mapping of chromosomal amplifications, deletions, and loss of heterozygosity (Mei et al., 2000; Bignell et al., 2004; Matsuzaki et al., 2004a,b; Wong et al., 2004; Zhao et al., 2004). The Affymetrix GeneChip Mapping 100K array set contains 116,204 SNP loci with a mean intermarker distance of 23.6 kb, and it enables detailed and genome-wide identification of DNA copy number changes (Matsuzaki et al., 2004a,b; Garraway et al., 2005; Zhao et al., 2005). The newer GeneChip Mapping 500K array set is composed of two arrays, each capable of genotyping an average 250,000 SNPs.

In the work reported here, we investigated DNA copy number aberrations in HCC cell lines using Affymetrix high-density SNP arrays. We identified a novel amplification at 17p11 in HCC cell lines. This region may harbor one or more genes that, when amplified, contribute to carcinogenesis. Within the amplicon, *MAPK7*, which encodes ERK5, emerged as a probable target gene that acts as a driving force for amplification of the region and promotes the growth of HCC cells by regulating entry into mitosis.

## MATERIALS AND METHODS

### Cell Lines and Tumor Samples

A total of 21 liver cancer cell lines [HCC-derived HLE, HLF (Dor et al., 1975), PLC/PRF/5 (Alexander et al., 1976), Li7 (Hirohashi et al., 1979), Huh7 (Nakabayashi et al., 1982), Hep3B (Aden et al., 1979), SNU354, SNU368, SNU387, SNU398, SNU423, SNU449, SNU475 (Park et al., 1995), JHH-1, JHH-2, JHH-4, JHH-5, JHH-6, JHH-7 (Fujise et al., 1990), Huh-1 (Huh et al., 1981), and the hepatoblastoma line HepG2 (Knowles et al., 1980)] were examined in this study. All cell lines were maintained in Dulbecco's modified Eagle's medium supplemented with 10% fetal bovine serum. We obtained 66 primary HCC tumors for analysis of the DNA copy number of *MAPK7* from patients undergoing surgery at the hospitals of Tokyo Medical and Dental University and Kyoto University, Japan. Genomic DNA was isolated from each cell line and from 66 primary tumors using the Puregene DNA isolation kit (Gentra, Minneapolis, MN). For immunohistochemical studies of ERK5, 43 additional HCC samples were obtained from the Hospital of Kyoto Prefectural University of Medicine, Japan. Before initiation of the present study, informed consent was obtained in the formal style approved by all relevant ethical committees.

### SNP Assay

The GeneChip Mapping 100K array set and GeneChip Mapping 250K Sty array (Affymetrix, Santa Clara, CA) were used in this study. Analyses were performed according to the manufacturer's instructions. In brief, 250 ng of genomic DNA was digested with a restriction enzyme (*Xba*I or *Hind*III for the 100K array set and *Sty*I for the 250K Sty array), ligated to an adaptor, and amplified by PCR (Kennedy et al., 2003; Matsuzaki et al., 2004a,b; Zhao et al., 2004). Amplified products were fragmented, labeled by biotinylation, and hybridized to the microarrays. Hybridization was detected by incubation with a streptavidin-phycoerythrin conjugate, followed by scanning of the array, and analysis was performed as described previously (Kennedy et al., 2003; Di et al., 2005). Copy number changes were calculated using the Copy Number Analyzer for Affymetrix GeneChip Mapping Arrays (http://www.genome.umin.jp) (Nannya et al., 2005).

### Fluorescence In Situ Hybridization

We performed FISH using the bacterial artificial chromosome (BAC) RP11-73E4 as a probe (Invitrogen, Carlsbad, CA) as described previously (Yasui et al., 2002). The BAC was selected

on the basis of its location according to the database provided by the UCSC (http://genome.ucsc.edu/). Briefly, the probe was labeled by nick translation with biotin-16-dUTP (Roche Diagnostics, Penzberg, Germany) and hybridized to metaphase chromosomes. Hybridization signals for biotin-labeled probes were detected with avidin-fluorescein (Roche Diagnostics).

### Real-Time Quantitative PCR

We quantified genomic DNA and mRNA using a real-time fluorescence detection method. Total RNA was obtained using Trizol (Invitrogen). Residual genomic DNA was removed by incubating the RNA samples with RNase-free DNase I (Takara Bio, Shiga, Japan) prior to reverse transcription (RT)-PCR. Single-stranded complementary DNA was generated using superscript III reverse transcriptase (Invitrogen) according to the manufacturer's directions. Real-time quantitative PCR experiments were performed with the LightCycler system using FastStart DNA Master Plus SYBR Green I (Roche Diagnostics) according to the manufacturer's protocol. The primers were as follows: *MAPK7* DNA (forward, 5′-TGCTGACTGGCTCGAAG-3′; reverse, 5′-GGGTCTGAGATGAACCTGC-3′); *MAPK7* mRNA (forward, 5′-TTTGCCTTACTTCCCACCTG-3′; reverse, 5′-CCCATGTCGAAAGACTGGTT-3′); *GRAP* mRNA (forward, 5′-TCGAAGGACAGACTGCACAC-3′; reverse, 5′-AGAAGAGGAGTGTGCCTCCA-3′); *EPN2* mRNA (forward, 5′-TCACCTCACCCACCACTGTA-3′; reverse, 5′-GTGGTCAGCTGCCCTTAGAG-3′); *EPPB9* mRNA (forward, 5′-CTTTGTGTACGGCCAGGACT-3′; reverse, 5′-CGTAGGGGTTGGTGCTTTTA-3′); *MFAP4* mRNA (forward, 5′-GGTGACTCCCTGTCCTACCA-3′; reverse, 5′-TCATCTCAGTGCGTTTGAGG-3′); *ZNF179* mRNA (forward, 5′-ACTGGGCAGAACCAGAGAGA-3′; reverse, 5′-AGGATGCACAGACAGGCTCT-3′); *FLJ10847* mRNA (forward, 5′-AACTCTTGGGCTTCAAGCAA-3′; reverse, 5′-AGGAGGTTGAGGCTGCAGTA -3′). These primers were designed using Primer3 (http://frodo.wi.mit.edu/cgi-bin/primer3/primer3_www.cgi) on the basis of sequence data obtained from the NCBI database (http://www.ncbi.nlm.nih.gov/). *GAPDH* (Minamiya et al., 2004) and long interspersed nuclear element (LINE)-1 (Zhao et al., 2004) were used as endogenous controls for mRNA and genomic DNA levels, respectively.

### Immunoblotting

Immunoblots were prepared according to previously reported methods (Yasui et al., 2001). Cell lysates (20 μg protein per sample) were separated by sodium dodecyl sulfate-polyacrylamide gel electrophoresis on 10% acrylamide gels. We obtained the following antibodies from Sigma-Aldrich (Tokyo, Japan): anti-ERK5 polyclonal antibody, anti-phospho-ERK5 (pThr218/pThr220) polyclonal antibody, and anti-β-actin monoclonal antibody. For immunoblotting, we used anti-ERK5, anti-phospho-ERK5, and anti-β-actin at dilutions of 1:500, 1:1000, and 1:5000, respectively. For secondary immunodetection, we used anti-rabbit or anti-mouse Ig (Amersham, Tokyo, Japan) diluted 1:5000. Protein binding was detected using the ECL system (Amersham).

### Immunoprecipitation

Cells were lysed with RIPA buffer (10 mM Tris-HCl, pH 7.4, 150 mM NaCl, 1% Triton X-100, 0.1% sodium dodecyl sulfate, 1% sodium deoxycholate, 1 mM phenylmethylsulfonyl fluoride), and incubated on ice for 30 min. The lysate was centrifuged at 14,000 × *g* at 4°C for 15 min. The supernatant was incubated with normal rabbit IgG and protein A-agarose beads (Santa Cruz Biotechnology, Santa Cruz, CA) to decrease nonspecific protein binding. After centrifugation, the supernatant was incubated with anti-ERK5 polyclonal antibody or normal rabbit IgG (control) overnight at 4°C. Protein A-agarose beads were added to the reaction and the mixture was incubated for an additional 1 hr. The precipitates were recovered by a brief centrifugation, followed by four washes with RIPA buffer. Samples were then boiled in electrophoresis sample buffer and separated by electrophoresis as described above (see "Immunoblotting" section).

### Immunohistochemical Analysis

Forty-three primary HCCs, consisting of paired tumor and surrounding nontumor tissues, and two HCC cell lines (SNU449 and Li7) were analyzed by anti-ERK5 immunostaining. Immunohistochemical staining was performed on formalin-fixed and paraffin-embedded sections using an anti-ERK5 polyclonal antibody (Sigma-Aldrich) at a 1:200 dilution. An automated tissue immunostainer (Ventana Medical Systems, Tucson, AZ) was used according to the manufacturer's instructions. The staining was developed with 3,3′-

diaminobenzidine tetrahydrochloride, followed by counterstaining with hematoxylin.

### Growth Assays and RNA Interference Studies

For cell growth assays viable cells were stained with 0.2% trypan blue and counted with a hemocytometer 24, 48, and 72 hr after transfection. For RNA interference (RNAi) studies, Stealth small interfering RNA (siRNA) duplex oligoribonucleotides targeting *MAPK7* (5′-CCAUGGCAUGAAC CCUGCCGAUAUU-3′) and Stealth RNAi negative control duplexes were synthesized by Invitrogen. The siRNAs were delivered into SNU449 cells using Lipofectamine 2000 (Invitrogen) according to the manufacturer's instructions. To determine mRNA levels, cells were harvested 48 hr after transfection and subjected to quantitative RT-PCR as described above.

### Cell Cycle Synchronization

SNU449 cells were synchronized at G1/S, early S, or M phases. For G1/S or early S-phase synchronization, cells were incubated in medium containing 2.5 mM thymidine (Sigma Chemical Co., St. Louis, MO) for 24 hr, followed by 12 hr in medium without thymidine, and finally another 12 hr in medium containing 2.5 mM thymidine (double-thymidine block; for G1/S-phase) or 1 μg/ml aphidicolin (early S-phase block). For M phase synchronization, cells were incubated in medium containing 2.5 mM thymidine for 24 hr, followed by 4 hr in medium without thymidine, and finally another 12 hr in medium containing 0.5 μg/ml nocodazole.

### Cell Cycle Analysis

SNU449 cells were synchronized at the G1/S-phase boundary by a double-thymidine block as described above. Synchronized cells were released into fresh medium without thymidine and harvested at the indicated time points. These cells were then stained with propidium iodide and analyzed using a FACSCaliber scanner and Cell Quest software (Becton Dickinson Pharmingen, San Diego, CA).

### Mitotic Index

Cells were grown in 24-well plates and transfected with Stealth RNAi targeting *MAPK7* or Stealth RNAi negative control duplexes as described above (see "Growth Assays and RNA Interference Studies" section). After 24 hr, cells were synchronized at the G1/S-phase boundary by a double-thymidine block. Synchronized cells were collected, reseeded on glass slides, and incubated for an additional 9 hr in fresh medium without thymidine. Next, the cells were stained with an anti-phospho-histone H3 antibody that specifically detects mitotic cells. Briefly, cells were fixed with 3.7% formaldehyde, permeabilized with 0.25% Triton X-100, and incubated with PBS containing 1% bovine serum albumin. The cells were then treated with a mixture of 4 μg/ml anti-phospho-histone H3 (Ser10)-biotin conjugated antibody (Upstate Biotechnology, Lake Placid, NY) and a 1:100 dilution of streptavidin-fluorescein (Roche Diagnostics) for 1 hr at room temperature, followed by counterstaining with propidium iodide. Positive staining for phospho-histone H3 was quantified by counting stained cells under a fluorescence microscope and dividing by the number of total cells. The mitotic index was scored as the percentage of mitotic cells in a population. On average, 200 cells were scored in three separate areas.

### Statistical Analysis

All statistical analyses were performed using SPSS 15.0 software (SPSS Inc., Chicago, IL). Chi-square tests or analysis of variance (ANOVA) were used. $P$ values $< 0.05$ were considered significant.

## RESULTS

### Detection of the 17p11 Amplicon in HCC Cell Lines by SNP Array Analysis

We screened for DNA copy number aberrations in 20 HCC cell lines by SNP array analysis. Two of the 20 cell lines, SNU449 and JHH-7, exhibited amplifications at chromosomal band 17p11 (Fig. 1A). In particular, the SNU449 cell line showed a high level of amplification in a narrow region on 17p11. We were able to define the smallest commonly affected region in the 17p11 amplicon as that lying between the positions recognized by the Affymetrix SNP_A-1662618 and SNP_A-1720748 probes (Fig. 1B). This region includes seven known or predicted protein-coding genes, *GRAP*, *EPN2*, *EPPB9*, *MAPK7*, *MFAP4*, *ZNF179*, and *FLJ10847*. The size of the amplicon was estimated to be approximately 750 kb.

To confirm amplification at 17p11 in SNU449 cells, we performed FISH analysis. The probe for

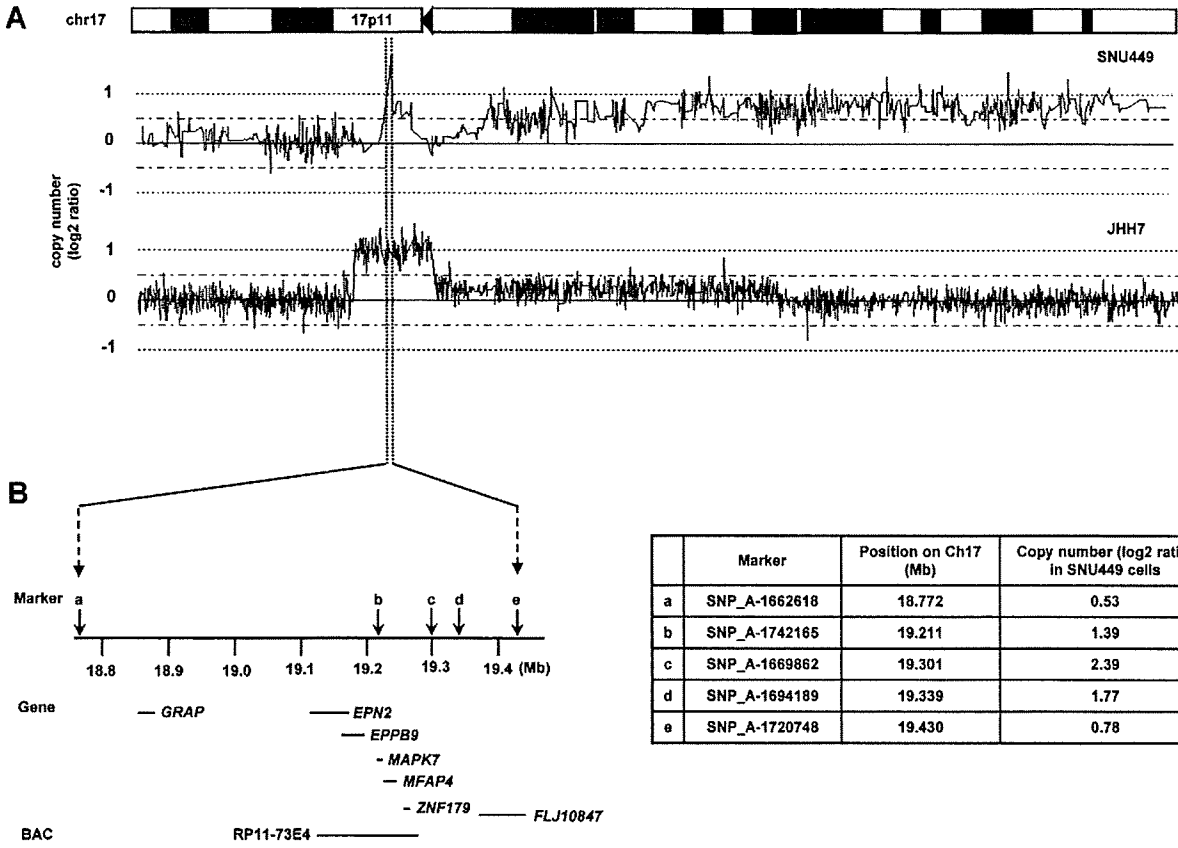


| | Marker | Position on Ch17 (Mb) | Copy number (log2 ratio) in SNU449 cells |
|---|---|---|---|
| a | SNP_A-1662618 | 18.772 | 0.53 |
| b | SNP_A-1742165 | 19.211 | 1.39 |
| c | SNP_A-1669862 | 19.301 | 2.39 |
| d | SNP_A-1694189 | 19.339 | 1.77 |
| e | SNP_A-1720748 | 19.430 | 0.78 |

Figure 1. Map of the amplicon at 17p11 in two HCC cell lines. A: Copy number profiles for chromosome 17 in SNU449 and JHH-7 cells. Copy number values were determined by SNP 100K and 250K array analyses for SNU449 and JHH-7 cells, respectively. B: The smallest common region of amplification in SNU449 and JHH-7 cells (left). The position of the Affymetrix SNP markers, the seven genes within the amplicon (*GRAP*, *EPN2*, *EPPB9*, *MAPK7*, *MFAP4*, *ZNF179*, and *FLJ10847*) and the BAC RP11-73E4 (used as a probe for FISH) are numbered according to the UCSC genome database (http://genome.ucsc.edu/). Detailed copy-number information at positions identified by individual SNP markers over the amplified region in SNU449 cells is shown at right.

these experiments was BAC RP11-73E4, which contains *EPN2*, *EPPB9*, *MAPK7*, *MFAP4*, and *ZNF179* (Fig. 1B). This probe showed an amplified FISH signal on metaphase chromosomes from SNU449 cells (Fig. 2A). To further characterize the relationship between the genes in this chromosomal region and amplifications observed in cancer cells, we analyzed the gene dosage of the *MAPK7* locus by real-time quantitative PCR of DNA from 21 different liver cancer cell lines (20 HCC cell lines and the hepatoblastoma line HepG2). Amplification of *MAPK7* was observed in SNU449 and JHH-7 cells (Fig. 2B). Taken together, the data provide strong evidence that the 17p11 region is amplified in SNU449 and JHH-7 cells.

### Analysis of Positional Candidate Genes in HCC Cell Lines

The 17p11 region may harbor one or more genes (henceforth referred to as "target genes") that, when activated by amplification, play a role in carcinogenesis. A common criterion for designating a gene as a putative target is that amplification leads to its overexpression (Collins et al., 1998). Thus, using real-time quantitative PCR, we determined the mRNA levels of all seven genes in the 17p11 amplicon in our panel of 21 liver cancer cell lines. As shown in Fig. 2C, the *EPN2*, *EPPB9*, and *MAPK7* genes were overexpressed in both SNU449 and JHH-7 cells. In several other lines, one or more of these three genes was overexpressed, despite the fact that regional amplification was not observed. These findings suggest that *EPN2*, *EPPB9*, and *MAPK7* are candidate target genes for 17p11 amplification.

Of these three genes, we chose to focus further analysis on *MAPK7*, which encodes ERK5, because ERK5-related proteins have been previously implicated in carcinogenesis (Hayashi and Lee, 2004; Wang and Tournier, 2006), whereas there is little or no evidence linking *EPN2* or

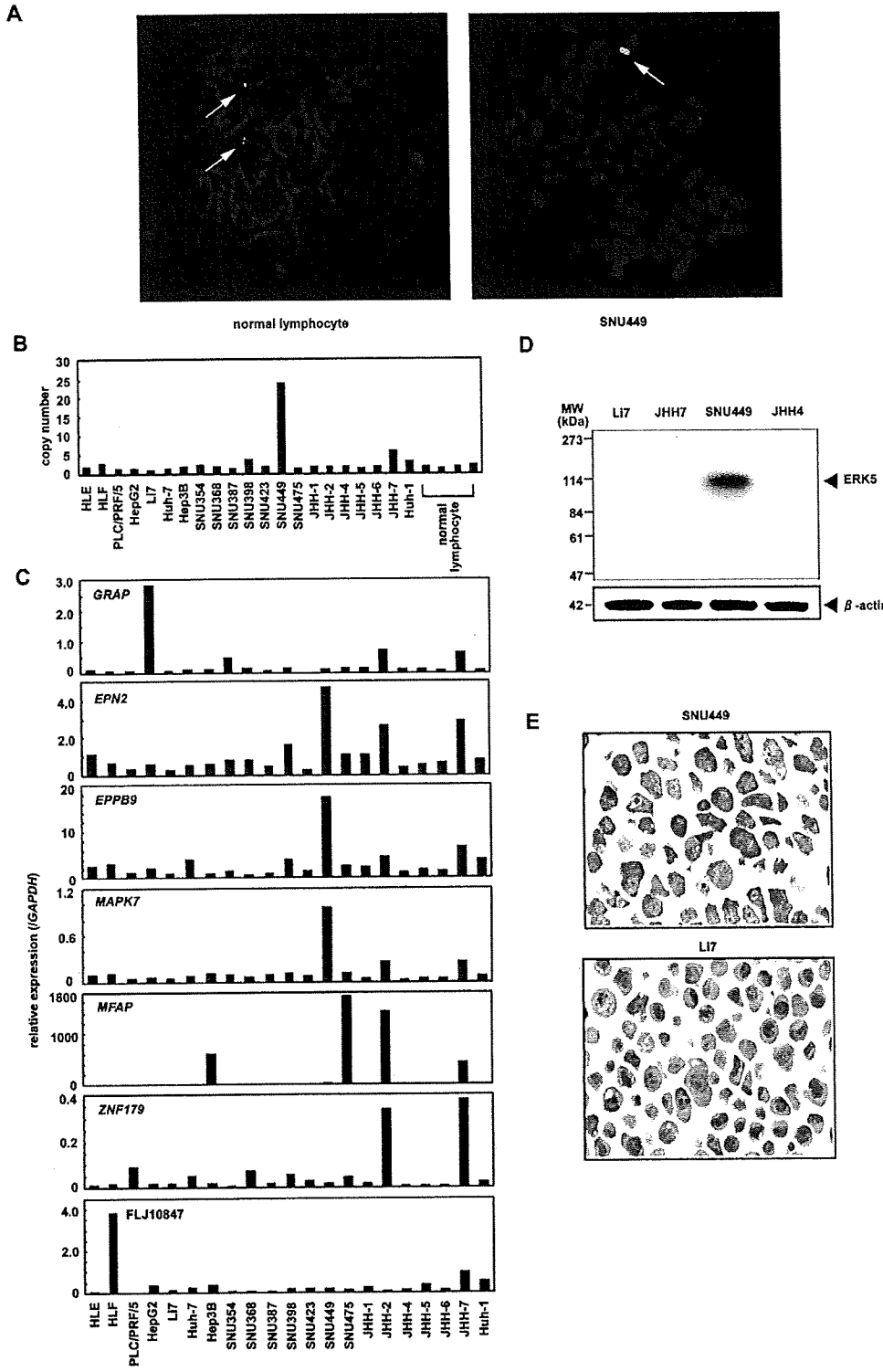


Figure 2. Amplification and overexpression of *MAPK7* in HCC cell lines. (A) Representative images from FISH analysis using a BAC RP11-73E4 probe on metaphase chromosomes from normal lymphocytes and SNU449 cells. While the probe shows a normal signal pattern (2 copies/cell) in normal lymphocytes (arrows, left), it shows an amplified signal in SNU449 cells (arrow, right). (B) Copy number of *MAPK7* in 21 liver cancer cell lines (20 HCC cells and one hepatoblastoma line, HepG2) and four peripheral blood lymphocytes (normal cell controls) as measured by real-time quantitative PCR with reference to a LINE-1 control. Values were normalized such that the average copy number of *MAPK7* in genomic DNA derived from normal lymphocytes is 2. (C) Relative expression levels of the seven genes within the 17p11 amplicon in a panel of 21 liver cancer cell lines as determined by real-time quantitative RT-PCR. The results are presented as the ratio between the expression level of each gene and a reference gene (*GAPDH*) to correct for variation in the amount of RNA. (D) Immunoblot analysis to detect protein levels of ERK5 and β-actin, an internal control, in four HCC cell lines with different *MAPK7* DNA copy numbers (B) and mRNA levels (C). (E) Immunostaining of ERK5 in SNU449 and Li7 cells.

*EPPB9* to tumorigenesis. Immunoblot analysis revealed that ERK5 expression is upregulated in SNU449 cells. Indeed, among the HCC cell lines that were tested, SNU449 showed the highest level of both 17p11 amplification and *MAPK7* overexpression (Fig. 2D). Moreover, immunostaining confirmed that the level of ERK5 was elevated in SNU449 cells. ERK5 was strongly expressed in the cytoplasm of SNU449 cells (Fig. 2E). In contrast, ERK5 was weakly expressed in only a few Li7 cells, a HCC cell line that shows neither amplification nor overexpression of *MAPK7* (Fig. 2E).

### Copy Number Gain of *MAPK7* in Primary HCC Tumors

To determine whether *MAPK7* is amplified in primary tumors, we examined 66 primary HCCs for copy number gains using real-time quantitative PCR. Copy number changes were counted as gains if the results of the analysis for a given tumor cell type exceeded the mean plus twice the standard deviation (SD) of the levels of *MAPK7* observed in genomic DNA derived from four peripheral blood lymphocyte samples (i.e., normal cells). A copy number gain for *MAPK7* was observed in 35 of the 66 tumors (53%; Fig. 3).

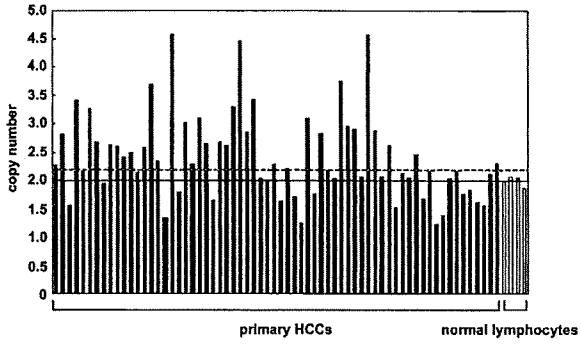


Figure 3. Copy number gain of *MAPK7* in primary HCC tumors. Copy numbers of *MAPK7* in 66 primary HCC tumors and four normal peripheral blood lymphocytes were determined by real-time quantitative PCR with reference to a LINE-1 control. Values were normalized such that the average copy number of *MAPK7* in genomic DNA derived from the normal lymphocytes equals 2 (solid horizontal line). The mean + 2 × SD of normal lymphocytes was used as the cutoff value for copy number gain (dotted line).

### Expression of ERK5 in Primary HCCs

We next examined the level of ERK5 in 43 additional primary HCCs, including paired tumor and surrounding nontumor tissues. Immunohistochemical studies revealed that, in nontumor tissues (normal liver, chronic hepatitis, or liver cirrhosis), ERK5 is strongly expressed in bile ducts, bile ductules, and a few small hepatocytes (Fig. 4A). In these cells, ERK5 was present in the cytoplasm. Hepatocytes also contained ERK5, although at a lower level than in bile ducts (Fig. 4A). The staining pattern for ERK5 was almost identical for normal liver, chronic hepatitis, and liver cirrhosis.

This granular cytoplasmic staining for ERK5 was also observed in HCC cancer cells (Fig. 4B). HCC cells containing ERK5 were uniformly distributed in the tumor tissues. The level of ERK5 was elevated in 11 of the 43 tumors compared with the paired nontumor tissues (Figs. 4B and 4C; Supp. Info. Table 1). To clarify the relationship between the level of ERK5 and various clinicopathological parameters, we examined available data from the 43 patients, whose tumors were divided into elevated (T>NT) and not elevated (T≤NT) groups. There was no significant correlation between the level of ERK5 and any parameter examined, including age and gender of the patients; size, stage, and degree of differentiation of the tumor; HBV or HCV infection; and

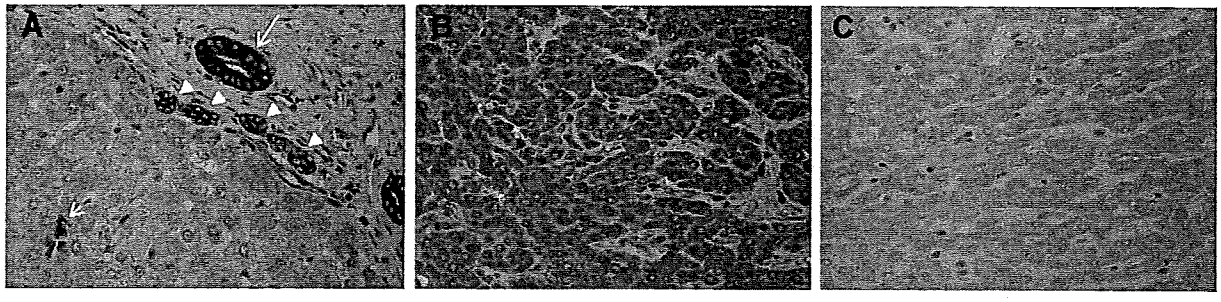


Figure 4. Representative ERK5 immunostaining of tissues. (A) A nontumorous liver tissue (chronic hepatitis). The level of ERK5 is elevated in the bile duct (large arrow), bile ductules (arrowheads), and a few small hepatocytes (small arrow). (B, C) Paired tumor (B) and nontumor (C) tissues from one HCC patient, wherein the level of ERK5 is elevated in the tumor compared with the counterpart nontumor tissue. Original magnification, ×400.

features of nontumorous liver tissues (Supp. Info. Table 1).

### Downregulation of *MAPK7* Inhibits the Growth of HCC Cells

To investigate the effects of *MAPK7* overexpression on HCC cells, we knocked down its expression using RNAi. In SNU449 cells treated with siRNA targeting *MAPK7*, we observed a decrease in *MAPK7* mRNA and ERK5 protein levels relative to that observed for cells receiving a control siRNA or transfection agent alone (Figs. 5A and 5B). The siRNA-mediated downregulation of *MAPK7* suppressed the growth of SNU449 cells at all time points assayed over a 72-hr period (Fig. 5C). These findings suggest that ERK5 promotes the growth of HCC cells.

### ERK5 is Phosphorylated During the G2/M Phases of the Cell Cycle

To help elucidate the underlying mechanism by which ERK5 regulates cellular proliferation we investigated the role of ERK5 in cell cycle progression. SNU449 cells were synchronized at G1/S, early S, or M phases of the cell cycle using a double-thymidine, aphidicolin, or nocodazole block, respectively. We determined the levels of total ERK5 and phosphorylated (active) form of ERK5. Immunoblotting did not show a difference in the level of total ERK5 among the three phases of the cell cycle (Fig. 6A). To detect phosphorylated ERK5, total ERK5 was immunoprecipitated from cell lysates using an anti-ERK5 antibody and then analyzed by immunoblotting using an anti-phospho-ERK5 antibody. Phosphorylated ERK5 was more abundant in cells synchronized at the M phase than in asynchronous cells (Fig. 6B).

We next synchronized SNU449 cells at the G1/S boundary using a double-thymidine block and then released the cells from the block. Using flow cytometry, we confirmed the synchrony of the cell cycle and monitored its progression after removal of thymidine (Fig. 6C). There was no difference in the level of total ERK5 during progression of the cell cycle (Fig. 6D). Expression of phosphorylated ERK was maximal 9 hr after release from the block (Fig. 6E), a time when a large proportion of cells were in the G2/M phase (Fig. 6C). Taken together, these observations indicate that ERK5 is phosphorylated during the G2/M phases of the cell cycle.

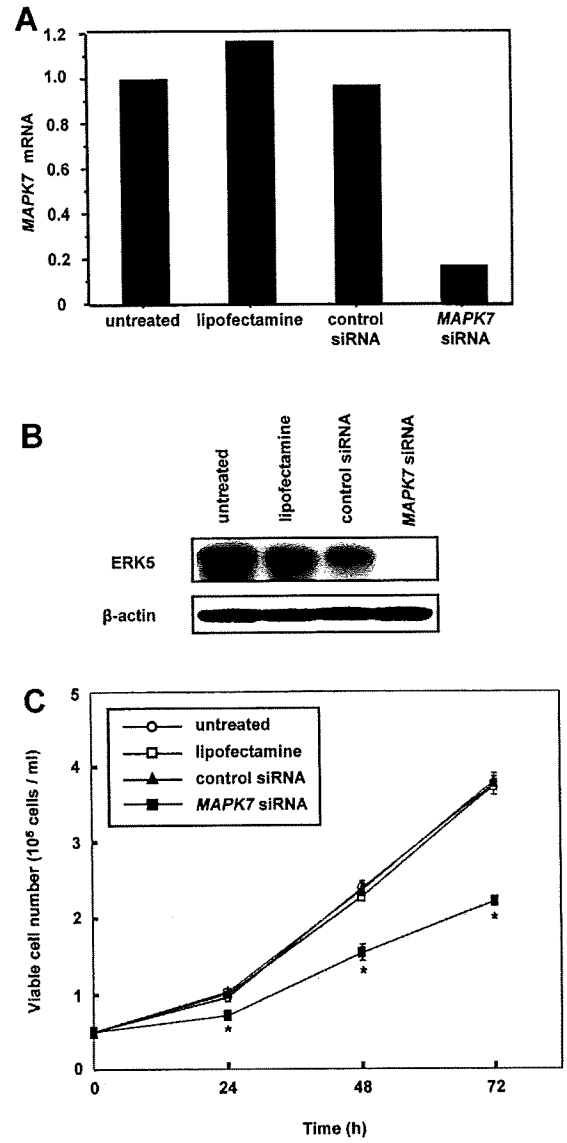


Figure 5. Growth inhibition of SNU449 cells by knockdown of *MAPK7*. A: Relative expression levels of *MAPK7* mRNA as determined by real-time quantitative RT-PCR. SNU449 cells were treated with siRNA targeting *MAPK7*, negative control siRNA, or the transfection agent alone (Lipofectamine), and harvested 48 hr after transfection. Untreated cells were maintained under identical experimental conditions. Results are presented as a ratio between the expression level of *MAPK7* and that of a reference gene (*GAPDH*) to correct for variation in the amount of RNA. Relative expression levels were normalized such that the ratio in untreated cells is 1. B: Levels of ERK5 and β-actin, an internal control, determined by immunoblotting. C: Cell growth was assayed by counting the viable cells at the indicated times after transfection. Each assay was performed in triplicate. Values are represented as the mean ± SD. Differences were analyzed by ANOVA (*$P < 0.01$).

### ERK5 Regulates Entry into Mitosis

Our results indicating that ERK5 is activated during the G2/M phases in SNU449 cells suggested that ERK5 may be involved in G2/M progression. To examine whether ERK5 plays a role in mitotic entry, we knocked down *MAPK7*

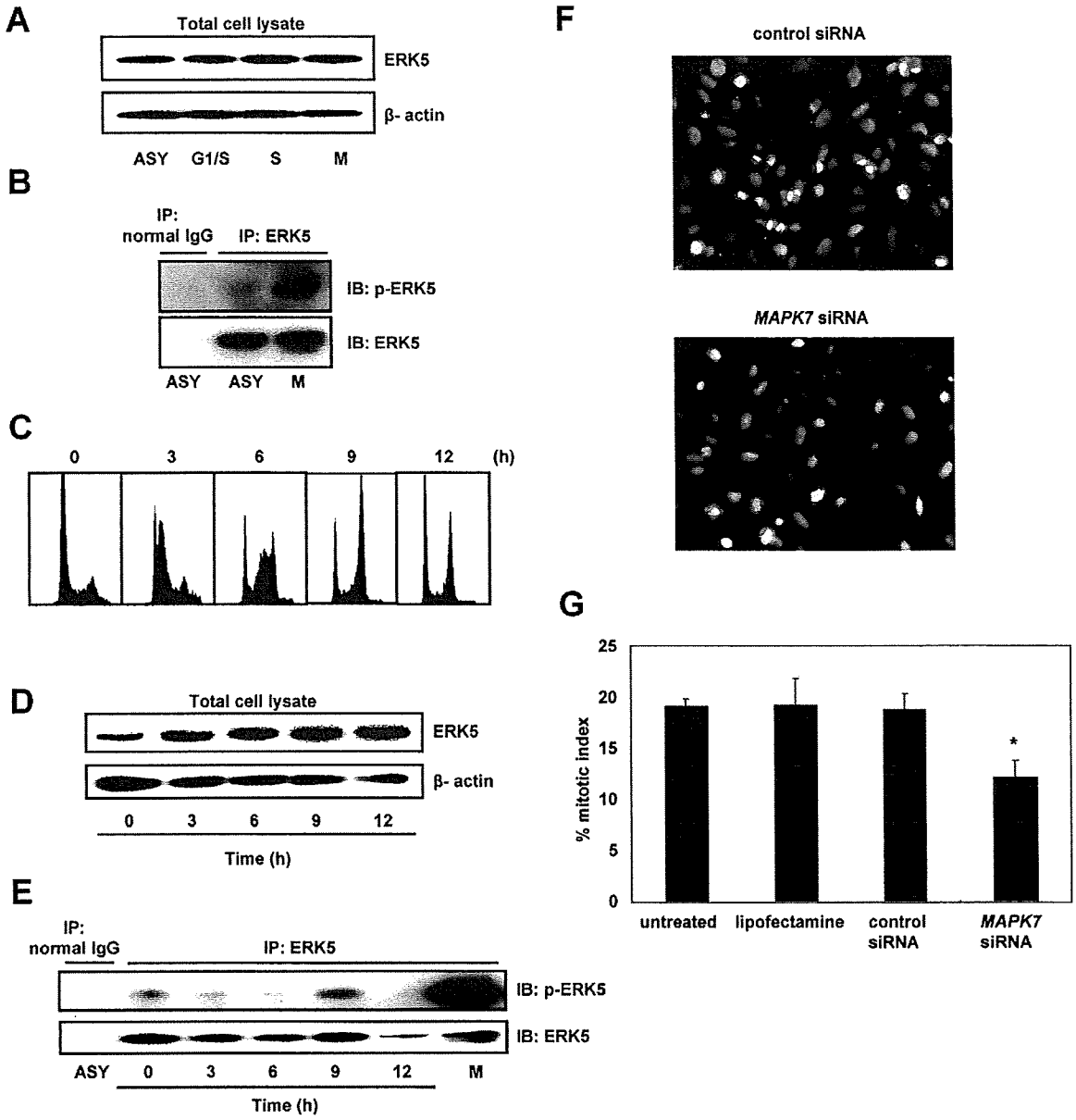


Figure 6. ERK5 is phosphorylated during the G2/M phases of the cell cycle. (A) Immunoblot analysis to detect protein levels of total ERK5 and β-actin, an internal control, in SNU449 cells that were synchronized at the G1/S, early S, or M phases using a double-thymidine, aphidicolin, or nocodazole block, respectively, or were untreated and used as an asynchronous (ASY) population. (B) Levels of phosphorylated ERK5 (p-ERK5). ERK5 was immunoprecipitated (IP) from lysates of SNU449 cells that were synchronized at the M phase (M) or from asynchronous cells (ASY). The samples were split and analyzed by immunoblotting (IB) for p-ERK5 and total ERK5. Normal rabbit immunoglobulin (normal IgG) was used as a negative control for immunoprecipitation. (C) Flow cytometric analysis. SNU449 cells were synchronized to the G1/S boundary using a double-thymidine block. Synchronized cells were released from the block and harvested at the indicated time points. The X-axis indicates DNA content and the Y-axis indicates the number of cells. (D) Time course of changes in the level of total ERK5 after release from the double-thymidine block. The level of β-actin was used as an internal control. (E) Time course of changes in the level of p-ERK5 after release from the double-thymidine block. ERK5 was immunoprecipitated from lysates of SNU449 cells harvested at the indicated times after release from the double-thymidine block. The samples were split and analyzed by immunoblotting for p-ERK5 and total ERK5. SNU449 cells, synchronized at the M phase with nocodazole, were also examined as described in (A) and (B). Normal rabbit IgG was used as a negative control for immunoprecipitation. (F) Representative images of mitotic cells in an SNU449 cell population that was transfected with *MAPK7*- or control-siRNA. SNU449 cells were treated with siRNA targeting *MAPK7*, negative control siRNA, or the transfection agent alone (Lipofectamine). Untreated cell were maintained under identical conditions. These cells were synchronized at the G1/S boundary using a double-thymidine block. The synchronized cells were released from the block and stained with anti-phospho-histone H3 9 hr after release, a time corresponding to the G2/M phase as shown in (C). Mitotic cells were identified by positive staining for phospho-histone H3 (green). Nuclear DNA was stained with propidium iodide (red). (G) The mitotic index was scored as described in Materials and Methods section. Data are presented as means ± SD (ANOVA; $^*P < 0.05$).

expression using RNAi and assessed its effect on mitosis. SNU449 cells were transfected with siRNA targeting *MAPK7* and synchronized at the G1/S-phase boundary by a double-thymidine block. The synchronized cells were released from the block and harvested 9 hr after release, a time which corresponds to the G2/M phase (Fig. 6C). Finally, harvested cells were stained with anti-phospho-histone H3 antibody, which specifically detects mitotic cells (Fig. 6F). Compared with a control siRNA or transfection agent alone, transfection of *MAPK7* siRNA significantly reduced the mitotic index (Fig. 6G). These findings suggest that ERK5 regulates mitotic entry in the HCC cells.

## DISCUSSION

High-density SNP arrays are powerful tools for high-resolution analysis of DNA copy number aberrations in cancers. In the present study, using the Affymetrix GeneChip 100K and 250K SNP arrays we detected a novel amplification in HCC cells at 17p11. We were able to narrow the amplification to a 750-kb region. Notably, the amplification might have been missed using conventional analyses such as CGH. Amplification at 17p11.2-p12 has been detected in high-grade osteosarcoma using CGH (Forus et al., 1995; Tarkkanen et al., 1995). The group of van Dartel et al., (2002) established 17p11.2-p12 amplification profiles by semi-quantitative PCR using 15 microsatellite markers and seven candidate genes to assay amplification in this tumor type. They found that most of the tumors had complex amplification profiles, suggesting that multiple amplification targets, including *MAPK7*, might be present in region 17p11.2-p12. In contrast, we were able to define a smaller common region of amplification at 17p11 in two HCC cells and to determine the expression status of all genes in the amplicon. Three of the seven genes in the amplicon; *EPN2*, *EPPB9*, and *MAPK7*, were always overexpressed in cells that showed amplification in the 17p11 region. Thus, we considered these three genes as candidate targets for amplification. The function of *EPPB9* (B9 protein) is not known, and the protein encoded by *EPN2* (epsin 2) is similar to epsin 1, which plays a putative role in clathrin-mediated endocytosis (Rosenthal et al., 1999). Therefore, we focused on *MAPK7* as a target for the amplification.

Several lines of evidence implicate ERK5, which is encoded by *MAPK7*, in tumorigenesis (Wang and Tournier, 2006): (a) the ERK5 pathway is activated by Ras (English et al., 1999), ErbB (Esparis-Ogando et al., 2002; Yuste et al., 2005), Src (Sun et al., 2003), Cot (Chiariello et al., 2000), Bcr-Abl (Buschbeck et al., 2005), insulin-like growth factor-II (Linnerth et al., 2005), and interleukin-6 (Carvajal-Vergara et al., 2005); (b) ERK5 is involved in the control of breast cancer cell proliferation (Esparis-Ogando et al., 2002); (c) ERK5 mediates a survival signal that confers chemoresistance to breast cancer (Weldon et al., 2002); (d) insulin-like growth factor-II promotes cell survival via the ERK5 pathway in lung cancer cells (Linnerth et al., 2005); (e) the level of ERK5 contributes to the survival of Bcr/Abl-positive leukemic cells (Buschbeck et al., 2005); (f) ERK5 regulates cell proliferation and antiapoptotic responses in multiple myeloma (Carvajal-Vergara et al., 2005); and (g) an elevated level of MEK5, a specific activator of ERK5, is associated with metastasis and a poor prognosis in prostate cancer (Mehta et al., 2003).

The present study is the first to show the status of amplification and expression of *MAPK7* and its functional role in HCC. We found that *MAPK7* is amplified in 35 of 66 HCC tumors (53%). However, we could not determine the copy number of *MAPK7* in the nontumorous counterparts of the samples assayed because these samples were not available. Therefore, we cannot exclude the possibility that copy number polymorphism might influence the results of copy number analysis. We studied the expression of ERK5 using immunohistochemical analysis in primary HCCs and their surrounding nontumorous liver tissues. In nontumorous liver tissues, ERK5 was weakly expressed in the cytoplasm of non-neoplastic hepatocytes. Intriguingly, it was more strongly expressed in bile ducts, bile ductules, and a few small hepatocytes. In HCC tumor tissues, ERK5 was expressed in the cytoplasm of tumor cells. The level of ERK5 was elevated in 11 of 43 HCC tumors compared with their nontumorous counterparts. However, we did not observe a significant link between the level of ERK5 and any clinicopathological parameters. A recent report showed that, in prostate cancer, an increase in ERK5 cytoplasmic signals correlates with advanced disease and that strong nuclear ERK5 localization correlates with poor survival (McCracken et al., 2008).

We examined the functional roles of ERK5 in HCC cells using RNAi. Downregulation of *MAPK7* by siRNA suppressed the growth of

SNU449 cells, which had the greatest amplification and overexpression of *MAPK7* of all of the cell lines tested. These findings suggest that increased levels of ERK5 enhance the growth of HCC cells. Moreover, our results indicate that ERK5 is phosphorylated during the G2/M phases of the cell cycle and that it regulates entry into mitosis, which may explain how it promotes the growth of HCC cells.

Conflicting results have been reported by different investigators regarding the role of ERK5 in cell cycle progression. Some investigators have reported that ERK5 regulates the G1/S transition: expression of a dominant-negative form of ERK5 prevents cells from entering the S-phase of the cell cycle (Kato et al., 1998), and ERK5 can drive cyclin D1 expression (Mulloy et al., 2003). In contrast, Cude et al., (2007) and Gírio et al., (2007) recently reported that ERK5 is activated at the G2/M phases and is required for mitotic entry, findings that agree with our results.

Few molecules have been identified as direct downstream targets of ERK5. The transcriptional factors of the monocyte enhancer factor 2 family are among the best characterized substrates of ERK5. Phosphorylation of monocyte enhancer factor 2C by ERK5 enhances its transcriptional activity and subsequently leads to an increase in c-Jun gene expression (Kato et al., 1997; Wang and Tournier, 2006). A more complete identification of components downstream of ERK5 will be necessary to fully understand the role of ERK5 in carcinogenesis.

In summary, using high-density SNP arrays, we identified *MAPK7* as a probable target for the amplification events at 17p11 in HCCs. Our results suggest that the ERK5 protein product of the *MAPK7* gene plays a role in proliferation of HCC cells by regulating mitotic entry and may therefore be an optimal target for the development of novel therapies for this widespread type of cancer.

## REFERENCES


Aden DP, Fogel A, Plotkin S, Damjanov I, Knowles BB. 1979. Controlled synthesis of HBsAg in a differentiated human liver carcinoma-derived cell line. Nature 282:615–616.

Alexander JJ, Bey EM, Geddes EW, Lecatsas G. 1976. Establishment of a continuously growing cell line from primary carcinoma of the liver. S Afr Med J 50:2124–2128.

Bignell GR, Huang J, Greshock J, Watt S, Butler A, West S, Grigorova M, Jones KW, Wei W, Stratton MR, Futreal PA, Weber B, Shapero MH, Wooster R. 2004. High-resolution analysis of DNA copy number using oligonucleotide microarrays. Genome Res 14:287–295.

Buschbeck M, Hofbauer S, Di Croce L, Keri G, Ullrich A. 2005. Abl-kinase-sensitive levels of ERK5 and its intrinsic basal activity contribute to leukaemia cell survival. EMBO Rep 6:63–69.

Carvajal-Vergara X, Tabera S, Montero JC, Esparís-Ogando A, López-Pérez R, Mateo G, Gutiérrez N, Parmo-Cabañas M, Teixidó J, San Miguel JF, Pandiella A. 2005. Multifunctional role of Erk5 in multiple myeloma. Blood 105:4492–4499.

Chiariello M, Marinissen MJ, Gutkind JS. 2000. Multiple mitogen-activated protein kinase signaling pathways connect the cot oncoprotein to the c-jun promoter and to cellular transformation. Mol Cell Biol 20:1747–1758.

Collins C, Rommens JM, Kowbel D, Godfrey T, Tanner M, Hwang SI, Polikoff D, Nonet G, Cochran J, Myambo K, Jay KE, Froula J, Cloutier T, Kuo WL, Yaswen P, Dairkee S, Giovanola J, Hutchinson GB, Isola J, Kallioniemi OP, Palazzolo M, Martin C, Ericsson C, Pinkel D, Albertson D, Li WB, Gray JW. 1998. Positional cloning of ZNF217 and NABC1: Genes amplified at 20q13.2 and overexpressed in breast carcinoma. Proc Natl Acad Sci USA 95:8703–8708.

Cude K, Wang Y, Choi HJ, Hsuan SL, Zhang H, Wang CY, Xia Z. 2007. Regulation of the G2-M cell cycle progression by the ERK5-NFkappaB signaling pathway. J Cell Biol 177:253–264.

Di Fiore PP, Pierce JH, Kraus MH, Segatto O, King CR, Aaronson SA. 1987. erbB-2 is a potent oncogene when overexpressed in NIH/3T3 cells. Science 237:178–182.

Di X, Matsuzaki H, Webster TA, Hubbell E, Liu G, Dong S, Bartell D, Huang J, Chiles R, Yang G, Shen MM, Kulp D, Kennedy GC, Mei R, Jones KW, Cawley S. 2005. Dynamic model based algorithms for screening and genotyping over 100 K SNPs on oligonucleotide microarrays. Bioinformatics 21:1958–1963.

Dor I, Namba M, Sato J. 1975. Establishment and some biological characteristics of human hepatoma cell lines. Gann 66:385–392.

El-Serag HB. 2002. Hepatocellular carcinoma: An epidemiologic view. J Clin Gastroenterol 35:S72–S78.

English JM, Pearson G, Hockenberry T, Shivakumar L, White MA, Cobb MH. 1999. Contribution of the ERK5/MEK5 pathway to Ras/Raf signaling and growth control. J Biol Chem 274:31588–1592.

Esparis-Ogando A, Diaz-Rodriguez E, Montero JC, Yuste L, Crespo P, Pandiella A. 2002. Erk5 participates in neuregulin signal transduction and is constitutively active in breast cancer cells overexpressing ErbB2. Mol Cell Biol 22:270–285.

Forus A, Weghuis DO, Smeets D, Fodstad O, Myklebost O, Geurts van Kessel A. 1995. Comparative genomic hybridization analysis of human sarcomas. II. Identification of novel amplicons at 6p and 17p in osteosarcomas. Genes Chromosomes Cancer 14:15–21.

Fujise K, Nagamori S, Hasumura S, Homma S, Sujino H, Matsuura T, Shimizu K, Niiya M, Kameda H, Fujita K. 1990. Integration of hepatitis B virus DNA into cells of six established human hepatocellular carcinoma cell lines. Hepatogastroenterology 37:457–460.

Garaude J, Cherni S, Kaminski S, Delepine E, Chable-Bessia C, Benkirane M, Borges J, Pandiella A, Iñiguez MA, Fresno M, Hipskind RA, Villalba M. 2006. ERK5 activates NF-kappaB in leukemic T cells and is essential for their growth in vivo. J Immunol 177:7607–7617.

Garraway LA, Widlund HR, Rubin MA, Getz G, Berger AJ, Ramaswamy S, Beroukhim R, Milner DA, Granter SR, Du J, Lee C, Wagner SN, Li C, Golub TR, Rimm DL, Meyerson ML, Fisher DE, Sellers WR. 2005. Integrative genomic analyses identify MITF as a lineage survival oncogene amplified in malignant melanoma. Nature 436:117–122.

Gírio A, Montero JC, Pandiella A, Chatterjee S. 2007. Erk5 is activated and acts as a survival factor in mitosis. Cell Signal 19:1964–1972.

Hayashi M, Lee JD. 2004. Role of the BMK1/ERK5 signaling pathway: Lessons from knockout mice. J Mol Med 82:800–808.

Hirohashi S, Shimosato Y, Kameya T, Koide T, Mukojima T, Taguchi Y, Kageyama K. 1979. Production of -fetoprotein and normal serum proteins by xenotransplanted human hepatomas in relation to their growth and morphology. Cancer Res 39: 1819–1828.

Huh N, Utakoji T. 1981. Production of HBs-antigen by two new human hepatoma cell lines and its enhancement by dexamethasone. Gann 72:178–179.

Kallioniemi A, Kallioniemi OP, Sudar D, Rutovitz D, Gray JW, Waldman F, Pinkel D. 1992. Comparative genomic hybridization for molecular cytogenetic analysis of solid tumors. Science 258:818–821.

Kato Y, Kravchenko VV, Tapping RI, Han J, Ulevitch RJ, Lee JD. 1997. BMK1/ERK5 regulates serum-induced early gene expression through transcription factor MEF2C. EMBO J 16:7054–7066.

Kato Y, Tapping RI, Huang S, Watson MH, Ulevitch RJ, Lee JD. 1998. Bmk1/Erk5 is required for cell proliferation induced by epidermal growth factor. Nature 395:713–716.

Kennedy GC, Matsuzaki H, Dong S, Liu WM, Huang J, Liu G, Su X, Cao M, Chen W, Zhang J, Liu W, Yang G, Di X, Ryder T, He Z, Surti U, Phillips MS, Boyce-Jacino MT, Fodor SP, Jones KW. 2003. Large-scale genotyping of complex DNA. Nat Biotechnol 21:1233–1237.

Knowles BB, Howe CC, Aden DP. 1980. Human hepatocellular carcinoma cell lines secrete the major plasma proteins and hepatitis B surface antigen. Science 209:97–499.

Linnerth NM, Baldwin M, Campbell C, Brown M, McGowan H, Moorehead RA. 2005. IGF-II induces CREB phosphorylation and cell survival in human lung cancer cells. Oncogene 24:7310–7319.

Little CD, Nau MM, Carney DN, Gazdar AF, Minna JD. 1983. Amplification and expression of the c-myc oncogene in human lung cancer cell lines. Nature 306:194–196.

Matsuzaki H, Dong S, Loi H, Di X, Liu G, Hubbell E, Law J, Berntsen T, Chadha M, Hui H, Yang G, Kennedy GC, Webster TA, Cawley S, Walsh PS, Jones KW, Fodor SP, Mei R. 2004a. Genotyping over 100,000 SNPs on a pair of oligonucleotide arrays. Nat Methods 1:109–111.

Matsuzaki H, Loi H, Dong S, Tsai YY, Fang J, Law J, Di X, Liu WM, Yang G, Liu G, Huang J, Kennedy GC, Ryder TB, Marcus GA, Walsh PS, Shriver MD, Puck JM, Jones KW, Mei R. 2004b. Parallel genotyping of over 10,000 SNPs using a one-primer assay on a high-density oligonucleotide array. Genome Res 14:414–425.

McCracken SR, Ramsay A, Heer R, Mathers ME, Jenkins BL, Edwards J, Robson CN, Marquez R, Cohen P, Leung HY. 2008. Aberrant expression of extracellular signal-regulated kinase 5 in human prostate cancer. Oncogene 27:2978–2988.

Mehta PB, Jenkins BL, McCarthy L, Thilak L, Robson CN, Neal DE, Leung HY. 2003. MEK5 overexpression is associated with metastatic prostate cancer, and stimulates proliferation, MMP-9 expression and invasion. Oncogene 22:1381–1389.

Mei R, Galipeau PC, Prass C, Berno A, Ghandour G, Patil N, Wolff RK, Chee MS, Reid BJ, Lockhart DJ. 2000. Genome-wide detection of allelic imbalance using human SNPs and high-density DNA arrays. Genome Res 10:1126–1137.

Minamiya Y, Matsuzaki I, Sageshima M, Saito H, Taguchi K, Nakagawa T, Ogawa J. 2004. Expression of tissue factor mRNA and invasion of blood vessels by tumor cells in non-small cell lung cancer. Surg Today 34:1–5.

Mulloy R, Salinas S, Philips A, Hipskind RA. 2003. Activation of cyclin D1 expression by the ERK5 cascade. Oncogene 22:5387–5398.

Nakabayashi H, Taketa K, Miyano K, Yamane T, Sato J. 1982. Growth of human hepatoma cells lines with differentiated functions in chemically defined medium. Cancer Res 42:3858–3863.

Nannya Y, Sanada M, Nakazaki K, Hosoya N, Wang L, Hangaishi A, Kurokawa M, Chiba S, Bailey DK, Kennedy GC, Ogawa S. 2005. A robust algorithm for copy number detection using high-density oligonucleotide single nucleotide polymorphism genotyping arrays. Cancer Res 65:6071–6079.

Nishimoto S, Nishida E. 2006. MAPK signalling: ERK5 versus ERK1/2. EMBO Rep 7:782–786.

Okamoto H, Yasui K, Zhao C, Arii S, Inazawa J. 2003. PTK2 and EIF3S3 genes may be amplification targets at 8q23-q24 and are associated with large hepatocellular carcinomas. Hepatology 38:1242–1249.

Park JG, Lee JH, Kang MS, Park KJ, Jeon YM, Lee HJ, Kwon HS, Park HS, Yeo KS, Lee KU, Kim ST, Chung JK, Hwang YJ, Lee HS, Kim CY, Lee YI, Chen TR, Hay RJ, Song SY, Kim WH, Kim CW, Kim YI. 1995. Characterization of cell lines established from human hepatocellular carcinoma. Int J Cancer 62:276–282.

Rosenthal JA, Chen H, Slepnev VI, Pellegrini L, Salcini AE, Di Fiore PP, De Camilli P. 1999. The epsins define a family of proteins that interact with components of the clathrin coat and contain a new protein module. J Biol Chem 274:33959–33965.

Sun W, Wei X, Kesavan K, Garrington TP, Fan R, Mei J, Anderson SM, Gelfand EW, Johnson GL. 2003. MEK kinase 2 and the adaptor protein Lad regulate extracellular signal-regulated kinase 5 activation by epidermal growth factor via Src. Mol Cell Biol 23:2298–2308.

Tarkkanen M, Karhu R, Kallioniemi A, Elomaa I, Kivioja AH, Nevalainen J, Böhling T, Karaharju E, Hyytinen E, Knuutila S, Kallioniemi OP. 1995. Gains and losses of DNA sequences in osteosarcomas by comparative genomic hybridization. Cancer Res 55:1334–1338.

van Dartel M, Cornelissen PW, Redeker S, Tarkkanen M, Knuutila S, Hogendoorn PC, Westerveld A, Gomes I, Bras J, Hulsebos TJ. 2002. Amplification of 17p11.2 approximately p12, including PMP22, TOP3A, and MAPK7, in high-grade osteosarcoma. Cancer Genet Cytogenet 139:91–96.

Wang X, Tournier C. 2006. Regulation of cellular functions by the ERK5 signalling pathway. Cell Signal 18:753–760.

Weldon CB, Scandurro AB, Rolfe KW, Clayton JL, Elliott S, Butler NN, Melnik LI, Alam J, McLachlan JA, Jaffe BM, Beckman BS, Burow ME. 2002. Identification of mitogen-activated protein kinase kinase as a chemoresistant pathway in MCF-7 cells by using gene expression microarray. Surgery 132:293–301.

Wong KK, Tsang YT, Shen J, Cheng RS, Chang YM, Man TK, Lau CC. 2004. Allelic imbalance analysis by high-density single-nucleotide polymorphic allele (SNP) array with whole genome amplified DNA. Nucleic Acids Res 32:e69.

Yasui K, Arii S, Zhao C, Imoto I, Ueda M, Nagai H, Emi M, Inazawa J. 2002. TFDP1, CUL4A, and CDC16 identified as targets for amplification at 13q34 in hepatocellular carcinomas. Hepatology 35:1476–1484.

Yasui K, Imoto I, Fukuda Y, Pimkhaokham A, Yang ZQ, Naruto T, Shimada Y, Nakamura Y, Inazawa J. 2001. Identification of target genes within an amplicon at 14q12-q13 in esophageal squamous cell carcinoma. Genes Chromosomes Cancer 32:112–118.

Yokoi S, Yasui K, Iizasa T, Imoto I, Fujisawa T, Inazawa J. 2003. TERC identified as a probable target within the 3q26 amplicon that is detected frequently in non-small cell lung cancers. Clin Cancer Res 9:4705–4713.

Yokoi S, Yasui K, Saito-Ohara F, Koshikawa K, Iizasa T, Fujisawa T, Terasaki T, Horii A, Takahashi T, Hirohashi S, Inazawa J. 2002. A novel target gene, SKP2, within the 5p13 amplicon that is frequently detected in small cell lung cancers. Am J Pathol 161:207–216.

Yuste L, Montero JC, Esparis-Ogando A, Pandiella A. 2005. Activation of ErbB2 by overexpression or by transmembrane neuregulin results in differential signaling and sensitivity to herceptin. Cancer Res 65:6801–6810.

Zhao X, Li C, Paez JG, Chin K, Jänne PA, Chen TH, Girard L, Minna J, Christiani D, Leo C, Gray JW, Sellers WR, Meyerson M. 2004. An integrated view of copy number and allelic alterations in the cancer genome using single nucleotide polymorphism arrays. Cancer Res 64:3060–3071.

Zhao X, Weir BA, LaFramboise T, Lin M, Beroukhim R, Garraway L, Beheshti J, Lee JC, Naoki K, Richards WG, Sugarbaker D, Chen F, Rubin MA, Jänne PA, Girard L, Minna J, Christiani D, Li C, Sellers WR, Meyerson M. 2005. Homozygous deletions and chromosome amplifications in human lung carcinomas revealed by single nucleotide polymorphism array analysis. Cancer Res 65:5561–5570.

# Association of Gankyrin Protein Expression with Early Clinical Stages and Insulin-Like Growth Factor-Binding Protein 5 Expression in Human Hepatocellular Carcinoma

Atsushi Umemura,[1,2] Yoshito Itoh,[2] Katsuhiko Itoh,[1] Kanji Yamaguchi,[2] Tomoki Nakajima,[2] Hiroaki Higashitsuji,[1] Hitoshi Onoue,[3] Manabu Fukumoto,[4] Takeshi Okanoue,[2] and Jun Fujita[1]

**Gankyrin (also known as PSMD10) is a liver oncoprotein that interacts with multiple proteins including MDM2 and accelerates degradation of the tumor suppressors p53 and Rb. We produced a monoclonal anti-gankyrin antibody and immunohistochemically assessed the clinicopathological significance of gankyrin overexpression in 43 specimens of human hepatocellular carcinoma (HCC). Specific cytoplasmic staining for gankyrin was observed in 62.8% (27/43) of HCCs, which was significantly associated with low TNM stage ($P = 0.004$), no capsular invasion ($P = 0.018$), no portal venous invasion ($P = 0.008$), and no intrahepatic metastasis ($P = 0.012$). The cumulative survival rate of patients with gankyrin-positive HCC was significantly higher than that with gankyrin-negative HCC ($P = 0.037$). p53 and MDM2 were positively stained by antibodies in 30.2% and 23.3%, respectively, of HCCs, but neither was inversely associated with gankyrin expression. In the Huh-7 human HCC cell line, overexpression of gankyrin up-regulated expression of insulin-like growth factor binding protein 5 (IGFBP-5), whereas suppression of gankyrin expression by siRNA down-regulated it. Supression of IGFBP-5 expression inhibited proliferation of Huh-7 cells as well as U-2 OS osteosarcoma cells. In HCC specimens, positive staining for IGFBP-5 was observed by immunohistochemistry in 41.9% (18/43), and the level of expression was significantly correlated with that of gankyrin (*rho* = 0.629, $P < 0.001$). *Conclusion:* These results suggest that gankyrin plays an oncogenic role(s) mainly at the early stages of human hepatocarcinogenesis, and that IGFBP-5 inducible by gankyrin overexpression may be involved in it.** (HEPATOLOGY 2008;47:493-502.)

Liver cancer is the sixth most common cancer worldwide (626,000 or 5.7% of new cancer cases) and the third most common cause of death from cancer (598,000) in 2002.[1] Eighty-two percent of cases are in developing countries, and the areas of high incidence are sub-Saharan Africa, eastern and southeastern Asia, and Melanesia. Histologically, more than 90% of the primary liver cancers are hepatocellular carcinomas (HCCs). Although there are several modalities of treatment for HCC, most patients present with unresectable tumors, and nonsurgical treatments are minimally effective at best.[2,3] Even for those patients who undergo surgical resection, the recurrence rate is very high and the prognosis is poor.[2,4-6] It is therefore important to clarify the mechanisms of human hepatocarcinogenesis and identify molecular targets to develop novel diagnostic, therapeutic, and preventive strategies.

By constructing subtracted complementary DNA (cDNA) libraries, we have previously identified 19 genes overexpressed in HCCs including 2 novel genes.[7,8] One of them was named gankyrin (gann-ankyrin repeat pro-

*Abbreviations: 3A6C2, mouse monoclonal anti-gankyrin antibody; cDNA, complementary DNA; HCC, hepatocellular carcinoma; IGF, insulinlike growth factor; IGFBP-5, insulin-like growth factor-binding protein 5; MDM2, mouse double minute 2; mRNA, messenger RNA; RT-PCR, reverse transcription polymerase chain reaction; siRNA, short interfering RNA; TNM, tumor-node-metastasis.*

*From the [1]Department of Clinical Molecular Biology, Graduate School of Medicine, Kyoto University, Kyoto, Japan; the [2]Molecular Gastroenterology and Hepatology, Graduate School of Medical Science, Kyoto Prefectural University of Medicine, Kyoto, Japan; the [3]Department of Nutritional Science, Faculty of Health and Welfare, Seinan Jo Gakuin University, Kitakyushu, Japan; and the [4]Department of Pathology, Institute of Development, Aging, and Cancer, Tohoku University, Sendai, Japan*

*Received May 21, 2007; accepted September 3, 2007.*

*Supported by Grants-in aid from the Ministry of Education, Culture, Sports, Science, and Technology of Japan and the Japan Society for the Promotion of Science.*

*Address reprint requests to: Jun Fujita, Department of Clinical Molecular Biology, Graduate School of Medicine, Kyoto University, 54 Shogoin Kawaharacho, Sakyo-ku, Kyoto 606-8507, Japan. E-mail: jfujita@virus.kyoto-u.ac.jp; fax: (81) 75-751-4977.*



*Published online in Wiley InterScience (www.interscience.wiley.com).*

*DOI 10.1002/hep.22027*

*Potential conflict of interest: Nothing to report.*

tein; "gann" in Japanese means cancer).[9] Gankyrin (also called PSMD10) consists of 7 ankyrin repeats, and its messenger RNA (mRNA) was overexpressed in 34 of 34 HCCs analyzed.[9,10] Independently, gankyrin was isolated as the p28 component or the interactor of the S6b subunit of the 19S regulator of the 26S proteasome.[11,12] The ankyrin repeat is the functional domain involved in protein–protein interactions, and gankyrin has been shown to interact with multiple proteins in addition to S6b. Gankyrin binds to retinoblastoma protein (Rb) and cyclin-dependent kinase (Cdk4), and accelerates phosphorylation and degradation of Rb, which results in release of the E2F transcription factor to activate DNA synthesis genes.[9,13] Gankyrin seems to play a role in cell cycle progression in noncancerous cells as well. Overexpression of gankyrin shortens population doubling time of NIH/3T3 mouse fibroblasts,[9] and its up-regulation correlates with cell cycle progression in normal rat primary hepatocytes, oval cells, and human hepatocytes.[14,15]

Overexpression of gankyrin confers tumorigenicity to NIH/3T3 cells and inhibits apoptosis in cultured human tumor cells exposed to chemotherapeutic agents.[10] The anti-apoptotic activity is attributable, at least partly, to increased degradation of p53, resulting in the reduced transcription of the p53-dependent proapoptotic genes.[16] Gankyrin binds to the E3 ubiquitin ligase MDM2 *in vitro* and *in vivo,* which increases p53–MDM2 association, thereby facilitating the ubiquitination and subsequent proteasomal degradation of p53 by MDM2. Gankyrin also controls MDM2 auto-ubiquitination and degradation, especially in the absence of p53.[16]

We produced a mouse monoclonal antibody against human gankyrin and assessed the expression of gankyrin protein in surgically resected HCC specimens by immunohistochemistry. Correlation of gankyrin positivity with clinicopathological findings and expression of p53 and MDM2 in HCC was analyzed. Furthermore, we demonstrated that expression of insulin-like growth factor-binding protein 5 (IGFBP-5) is inducible by overexpression of gankyrin in HCCs.

## Patients and Methods

***Patients and Specimens.*** HCC tissues and their corresponding noncancerous liver tissues were obtained from 43 and 32 patients, respectively, who had undergone curative hepatectomy at the University Hospital of Kyoto Prefectural University of Medicine between 1992 and 2000. The specimens used were routinely processed, formalin-fixed, and paraffin-embedded. After hematoxylin-eosin staining, all samples were diagnosed as HCC and the tumor-node-metastasis (TNM) classification was made according to the fourth edition of the general rules for the clinical and pathological study of primary liver cancer proposed by the Liver Cancer Study Group of Japan.[17] The demographic profiles of the patients are summarized in Table 1. For western blot analysis, HCCs and noncancerous liver tissues were obtained from 3 patients undergoing liver transplantation at the University Hospital of Kyoto Prefectural University of Medicine between 2004 and 2006. No donor organs were obtained from executed prisoners or other institutionalized persons. The study protocol conformed to the ethical guidelines of the 1975 Declaration of Helsinki and was approved by the institutional review boards. Written informed consents were obtained from all patients for subsequent use of their resected tissues.

**Table 1. Patient and Tumor Characteristics**

| Characteristic | Number (Percentage) |
|---|---|
| Number of patients | 43 |
| Sex distribution | |
| Male | 27 (62.8%) |
| Female | 16 (37.2%) |
| Age (years) | 25-78, median 65 |
| Virus marker | |
| HBV(+)/HCV(−) | 6 (14.0%) |
| HBV(−)/HCV(+) | 28 (65.0%) |
| HBV(+)/HCV(+) | 3 (7.0%) |
| HBV(−)/HCV(−) | 6 (14.0%) |
| AFP(ng/mL) | 3.5-39999, median 90 |
| Tumor size (cm) | 1.6-17.0, median 4.0 |
| Liver cirrhosis | |
| Yes | 29 (67.5%) |
| No | 14 (32.5%) |
| Chronic hepatitis | 13 (30.2%) |
| Normal | 1 (2.3%) |
| TNM stage | |
| I | 4 (9.3%) |
| II | 22 (51.1%) |
| III | 8 (18.6%) |
| IV | 9 (21.0%) |
| Histological differentiation | |
| Well | 12 (27.9%) |
| Moderate | 25 (58.1%) |
| Poor | 6 (14.0%) |
| Capsular formation | |
| Yes | 36 (83.7%) |
| No | 7 (16.3%) |
| Capsular invasion | |
| Yes | 14 (32.6%) |
| No | 29 (67.4%) |
| Portal venous invasion | |
| Yes | 9 (20.9%) |
| No | 34 (79.1%) |
| Intrahepatic metastasis | |
| Yes | 16 (37.2%) |
| No | 27 (62.8%) |

Abbreviations: HCV(+), anti-hepatitis C virus antibody positive; HBV(+), hepatitis B surface antigen positive; (−), negative; AFP, serum alpha-fetoprotein.

***Cell Culture and Transfection.*** Huh-7 human HCC cells, U-2 OS human osteosarcoma cells, 293T human embryonic kidney cells, mouse lymph node cells, and P3X63Ag8U.1 mouse myeloma cells were cultured in Dulbecco's modified Eagle's medium (Gibco BRL Life Technologies, NY) supplemented with 10% fetal bovine serum as described.[16] To assess viable cell numbers, we used the Dojindo Cell Counting Kit-8 (CCK8 kit, Dojindo Laboratories, Kumamoto, Japan) according to the manufacturer's instructions.

The 293T, Huh-7, and U-2 OS cells were transfected with plasmid DNA by using the calcium phosphate method or FuGENE 6 Transfection Reagent (Roche Diagnostics, Mannheim, Germany) as described.[16] Short interfering RNA (siRNA) were transfected at a final concentration of 25 nM by using siPORT NeoFX Transfection Agent (Ambion, Austin, TX) following the manufacturer's instructions. Twenty-four hours after transfection, the medium was replaced with fresh medium containing fetal bovine serum, and the culture was continued for another 24 or 48 hours. Then, the cells were harvested for analysis. All transfection assays were repeated at least 3 times.

***Plasmids and siRNA.*** Human wild-type gankyrin cDNAs, full coding sequence and deletion mutants, were cloned into the mammalian expression vector pMKIT-NEO and expressed as hemagglutinin (HA)-tagged proteins (Fig. 1A). Full-length gankyrin was expressed without a tag as well. To obtain recombinant human gankyrin protein, the full-length cDNA was cloned into an expression vector derived from pET28 (Novagen, EMD Biosciences Inc., San Diego, CA) and expressed as hexahistidine-tagged protein.

To down-regulate gene expression, Silencer Predesigned siRNAs for gankyrin (Ambion) and Stealth Select iRNA: for IGFBP-5 (Invitrogen, Tokyo, Japan), were used together with respective control RNAs.

***Antibodies.*** To obtain monoclonal antibodies against human gankyrin, recombinant (His)6-gankyrin protein was used as an immunogen. It was dissolved in phosphate-buffered saline (1 mg/mL) and emulsified with an equal volume of Freund's complete adjuvant (Difco, Becton-Dickinson, Franklin Lakes, NJ). Two female BALB/c mice were injected with the emulsion (50 $\mu$L/mouse) in the footpad. Two weeks after immunization, the inguinal lymph node cells ($4 \times 10^7$ cells) were fused with P3X63Ag8U.1 myeloma cells ($1 \times 10^7$) using polyethylene glycol 1500 (Roche Diagnostics). Fused cells were cultured in 96-well plates at $2 \times 10^5$ cell/well. The supernatants were assayed for the anti-gankyrin antibody titer by an enzyme-linked immunosorbent assay using recombinant His-tagged, glutathione-S-transferase (GST)-tagged, and nontagged gankyrin proteins. Selected relevant hybridomas were cloned by the limiting dilution method, and the isotypes of secreted monoclonal antibodies were determined by the IsoStrip kit (Roche Diagnostics) following the manufacturer's instructions. Finally, an IgG2b kappa monoclonal antibody that showed the highest affinity for gankyrin was obtained and named 3A6C2.

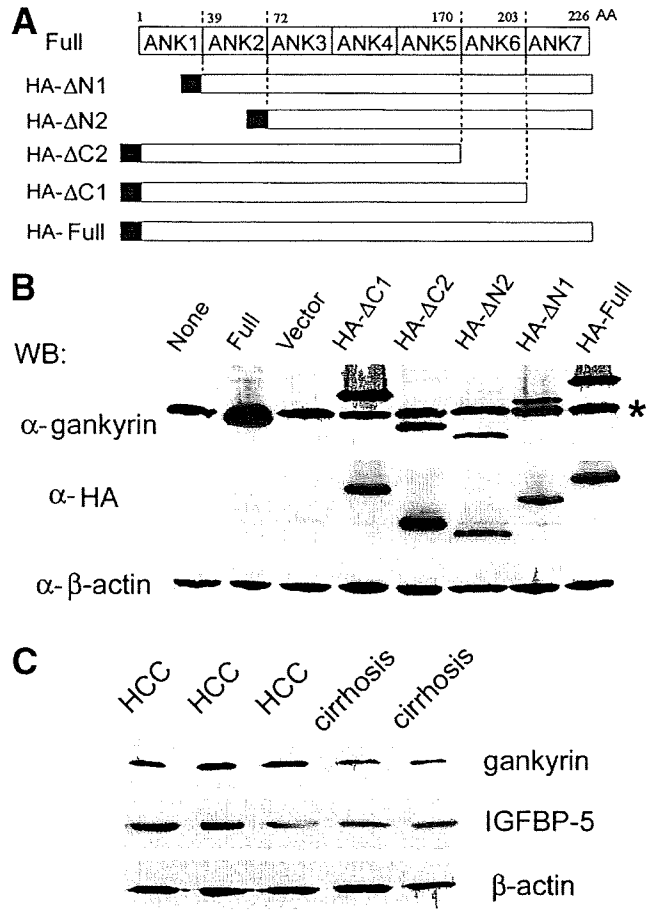


Fig. 1. Recognition of gankyrin protein by the monoclonal antibody. (A) Structures of wild-type gankyrin (Full) and its deletion mutants. Numbers on top, N- and C-terminal amino-acid residues. ANK, ankyrin repeat. Black bars, HA tags. (B) Specificity of the antibody. 293T cells were transfected with plasmids expressing the indicated proteins. Cell lysates were analyzed by western blotting (WB) using the anti-gankyrin monoclonal antibody (3A6C2), anti-HA antibody, and anti-$\beta$-actin antibody. *Mobility of the endogenous gankyrin. Representative results of 3 repeated experiments are shown. (C) Detection of gankyrin protein in tissues. Lysates were made from hepatocellular carcinoma (HCC, n = 3) and cirrhotic liver tissues (n = 2), and analyzed by WB using antibodies for indicated proteins. HA, hemagglutinin.

For western blot analysis, mouse monoclonal anti-gankyrin antibody (3A6C2), goat polyclonal anti–IGFBP-5 antibody (R&D Systems Inc., Minneapolis, MN), mouse monoclonal anti-HA antibody (12CA5, Roche Diagnostics), and mouse monoclonal anti–$\beta$-actin antibody (Chemicon International, Temecula, CA) were

used. Horseradish peroxidase–conjugated secondary antibodies against mouse or goat immunoglobulins were obtained from DAKO (Kyoto, Japan).

For immunohistochemistry, mouse monoclonal anti-gankyrin (3A6C2), anti-MDM2 (Ab-4, Oncogene research products, Boston, MA), and anti-p53 (DO-7, DAKO) antibodies, rabbit polyclonal anti-IGFBP-5 antibody (GroPep, Thebarton, Australia), and horseradish peroxidase–conjugated secondary antibodies against mouse or rabbit immunoglobulins (DAKO) were used.

***Analysis of Gene Expression.*** Extraction of RNA, preparation of cell and tissue lysates, and western blot analysis were performed as described.[9] Real-time reverse transcription polymerase chain reaction (RT-PCR) analysis was performed using ABI PRISM 7900 (Applied Biosystems, Foster City, CA) and a 1-step QuantiTect RT-PCR Kit (Qiagen, Cowley, UK) according to the manufacturer's instructions. PCR conditions were 50°C for 30 minutes and 95°C for 15 minutes, followed by 45 cycles of 95°C for 15 seconds, 55°C for 30 seconds, and 72°C for 45 seconds. Specific PCR amplification products were detected by SYBR Green. Transcripts of β-actin were quantified as control. Primer sequences used were as follows: IGFBP-5, AAGAAGCTGACCCAGTCCAA and GAATCCTTTGCGGTCACAAT; gankyrin, GCAACTTGGAGTGCCAGTGAA and TCACTTGAGCACCTTTTCCCA; β-actin, CTACGTCGCCCTGGACTTCGAGC and GATGGAGCCGCCGATCCACACGG.

The immunohistochemical staining was performed on 4-μm-thick paraffin sections of tissues fixed in buffered formalin. The sections were pretreated with 10 mM citrate buffer (pH 6.1) in a microwave oven for 5 minutes. Endogenous peroxidase activity was blocked with 0.3 % $H_2O_2$ for 10 minutes. The sections were incubated with 10% fetal bovine serum for 30 minutes to reduce nonspecific binding, followed by incubation with the primary antibody at 4°C overnight. They were subsequently incubated with horseradish peroxidase–conjugated anti-mouse or rabbit immunoglobulin antibody for 30 minutes. The enzymatic reaction was developed in a freshly prepared solution of 3,3′-diaminobenzidine tetrahydrochloride using DAKO Liquid DAB Substrate-Chromogen Solution for 10 minutes at room temperature. The sections were then counterstained with hematoxylin. The staining pattern, the distribution of the immunostaining in each tissue, and the intensity of the staining were studied in detail. Negative controls were conducted by substituting normal sera of each animal for the primary antibodies. When immunoreactivities were heterogenously observed, cases with moderate or strong staining of nucleus or cytoplasm in more than 5% of the cells were considered positive. To analyze the correlation of the expression levels of gankyrin and IGFBP-5, the staining intensity was expressed as 0 (negative), 1+ (weakly positive), 2+ (moderately positive), or 3+ (strongly positive). In each case the immunoreactivity was determined in 5 random high-powered fields and the count was done independently by 2 observers.

***Statistical Analysis.*** Categorical variables were compared using Fisher's exact test. Paired comparison of continuous data was performed using the Wilcoxon signed ranks test. To assess whether the 2 variables covary, Spearman's rank correlation coefficient was determined. Cumulative survival curves were calculated by the Kaplan-Meier method and analyzed by the log-rank test. All statistical analyses were performed using the JMP statistical software package (SAS Institute Inc., Cary, NC). A $P$ value less than 0.05 was considered statistically significant.

## Results

***Clinicopathological Profiles.*** Forty-three patients with HCC were recruited in this study, including 27 men and 16 women, with ages ranging from 25 to 78 (median 65) years old. Clinicopathological profiles of the patients and their HCCs are shown in Table 1. Antibody to hepatitis C virus was found in sera of 72% of the patients, and hepatitis B virus surface antigen was positive in 21%.

According to the TNM staging, 60% were stage I to II and 40% were stage III to IV. In noncancerous portions of the resected livers, cirrhosis and chronic hepatitis[18] were found in 68% and 30%, respectively, of the specimens, whereas only 1 (2%) was of normal histology. Fibrocapsular formation surrounding HCC was observed in 84% and capsular invasion by HCC cells in 33%. Portal vein involvement and satellite nodules suggesting intrahepatic metastasis were found in 21% and 37%, respectively.

***Detection of Gankyrin with the Monoclonal Anti-gankyrin Antibody.*** To determine the specificity of the monoclonal anti-gankyrin antibody 3A6C2, we expressed wild-type full-length or truncated gankyrin (Fig. 1A) in 293T cells. The antibody detected all mutants of gankyrin, suggesting that the epitope exists within the third and fifth ankyrin-repeat region (Fig. 1B). The antibody recognized the endogenous gankyrin as well, and no major cross-reacting band was observed.

Because gankyrin mRNA is known to be overexpressed in most HCCs,[9] we analyzed the levels of gankyrin protein in HCCs and surrounding noncancerous liver tissues using the 3A6C2 antibody. The protein level of gankyrin was higher in HCC tissues than in noncancerous tissues

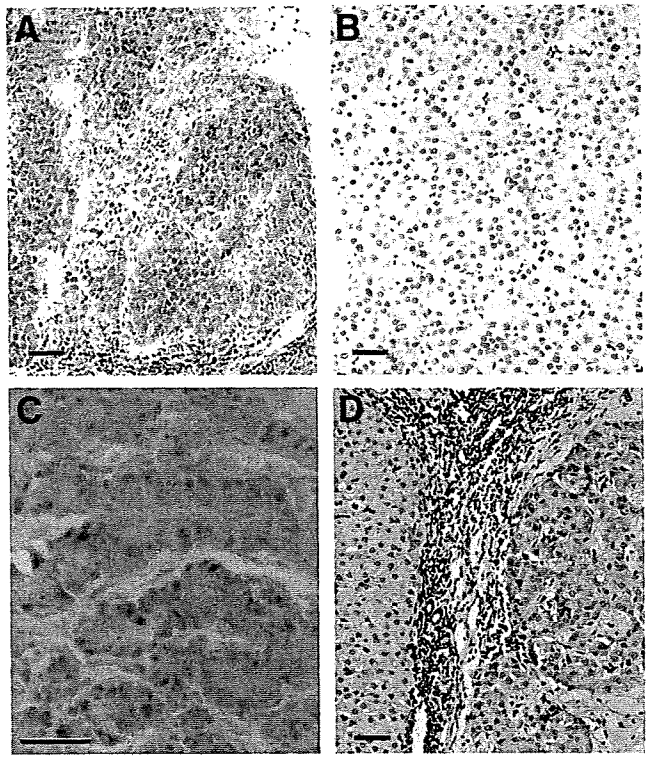


Fig. 2. Immunohistochemical detection of gankyrin in hepatocellular carcinoma (HCC). HCC sections were stained with mouse monoclonal anti-gankyrin antibody, and counterstained with hematoxylin. Positive immunostaining appears brown. (A) Positive staining for gankyrin in the cytoplasm of most HCC cells. (B) Barely detectable gankyrin signal in some HCC cells. (C) Presence of gankyrin in the nucleus of some HCC cells. (D) Stronger staining for gankyrin in HCC cells (right) than the neighboring cirrhotic hepatocytes (left). Bar, 50 $\mu$m.

(Fig. 1C). The mobilities of the gankyrin band were not different among samples.

***Immunohistochemical Analysis of Gankyrin Expression.*** We next examined the expression of gankyrin protein in HCC and noncancerous liver tissues by immunohistochemistry. The gankyrin signal was observed mainly in the cytoplasm and occasionally in the nucleus of HCC cells (Fig. 2A-C). Although at lower levels compared with those in HCCs, weak but reproducible gankyrin signals were observed in the cytoplasm of the hepatocytes in the noncancerous tissues (Fig. 2D). Expression of gankyrin was not detected in the bile duct cells, blood endothelial cells, or other nonparenchymal cells in the liver tissues. Of 43 HCCs examined, the cytoplasm was stained positively for gankyrin in 27 (63%), and 9 of them (21%) were also positive for nuclear staining. Of 32 noncancerous liver tissues available, gankyrin was positive in 17 (53%).

As shown in Table 2, we analyzed an association between gankyrin protein expression and clinicopathological findings. No significant association between gankyrin expression in HCC cells and sex, age, tumor size, fibrotic change in noncancerous liver tissues, differentiation of the tumor cells, or hepatitis B or C virus infection was observed. Positive cytoplasmic staining for gankyrin of HCC cells was significantly associated with low TNM stage (stage I or II; $P = 0.004$), no capsular invasion ($P = 0.018$), no portal venous invasion ($P = 0.008$), and no intrahepatic metastasis ($P = 0.012$) of HCC. In noncancerous liver tissues, positive gankyrin staining of hepatocytes was associated with the cytoplasmic gankyrin positivity of HCC cells of the same patient ($P = 0.021$, Table 3), but not with the parameters examined except for the serum alpha-fetoprotein level ($P = 0.015$, Table 2).

Because expression of gankyrin affects the degradation of p53 and MDM2,[16] we examined the expression of p53 and MDM2 as well as gankyrin in HCCs. By immunohistochemistry, nuclear expression of p53 and MDM2 were detected in 30% and 23%, respectively, of 43 HCCs (Fig. 3, Table 3). Positive staining for gankyrin was not associated with the staining for p53 nor MDM2 in HCC cells.

***Up-regulation of IGFBP-5 Expression by Gankyrin in HCCs.*** Preliminary microarray analysis of the cDNA libraries prepared from U-2 OS cells and Huh-7 cells overexpressing gankyrin suggested that IGFBP-5 mRNA was up-regulated by gankyrin (A. Umemura and J. Fujita, unpublished data). Real-time RT-PCR analysis con-

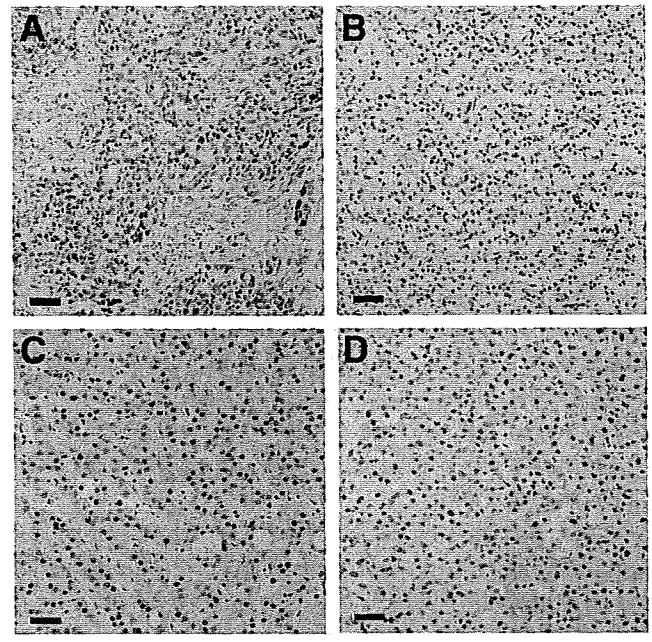


Fig. 3. Immunohistochemical detection of p53 and MDM2 in hepatocellular carcinoma (HCC). HCC sections were stained with antibodies specific to p53 (A and B) or MDM2 (C and D), and counterstained with hematoxylin. Positive immunostaining appears brown. (A) Positive staining for p53 in the nucleus of most HCC cells. (B) Negative p53 in HCC cells. (C) Positive staining for MDM2 in the nucleus of most HCC cells. (D) Negative MDM2 in HCC cells. Bar, 50 $\mu$m.

**Table 2. Gankyrin Expression and Clinicopathological Characteristics**

| | Gankyrin Expression in the Cytoplasm of | | | | | |
|---|---|---|---|---|---|---|
| | HCC | | | Noncancerous Liver | | |
| | Negative (n = 16) | Positive (n = 27) | *P* value | Negative (n = 15) | Positive (n = 17) | *P* value |
| Sex distribution | | | | | | |
| Male | 12 | 15 | 0.328 | 10 | 11 | 1.000 |
| Female | 4 | 12 | | 5 | 6 | |
| Median age (years) | 64 | 65 | 0.696 | 63 | 62 | 0.649 |
| Virus marker | | | NS | | | NS |
| HBV(+)/HCV(−) | 3 | 3 | | 2 | 2 | |
| HBV(−)/HCV(+) | 10 | 18 | | 11 | 11 | |
| HBV(+)/HCV(+) | 1 | 2 | | 2 | 0 | |
| HBV(−)/HCV(−) | 2 | 4 | | 0 | 4 | |
| Median AFP (ng/mL) | 63.0 | 95.0 | 0.890 | 25.0 | 199.0 | 0.015 |
| Median tumor size (cm) | 4.5 | 4.0 | 0.098 | 4.5 | 4.0 | 0.372 |
| Liver cirrhosis (+) | 9 | 20 | 0.316 | 9 | 13 | 0.450 |
| TNM stage | | | | | | |
| I and II | 5 | 21 | 0.004 | 8 | 12 | 0.467 |
| III and IV | 11 | 6 | | 7 | 5 | |
| Histological differentiation | | | | | | |
| Well | 5 | 7 | 0.737 | 6 | 3 | 0.243 |
| Moderate and poor | 11 | 20 | | 9 | 14 | |
| Capsular formation (+) | 15 | 21 | 0.229 | 12 | 13 | 1.000 |
| Capsular invasion (+) | 9 | 5 | 0.018 | 4 | 6 | 0.712 |
| Portal venous invasion (+) | 7 | 2 | 0.008 | 4 | 3 | 0.678 |
| Intrahepatic metastasis (+) | 10 | 6 | 0.012 | 6 | 5 | 0.712 |
| Gankyrin nuclear expression | | | | | | |
| Yes | 0 | 9 | 0.016 | 2 | 5 | 0.403 |
| No | 16 | 18 | | 13 | 12 | |

Abbreviations: HCV, anti-hepatitis C virus antibody; HBV, hepatitis B surface antigen; (+), positive or present; (−), negative or absent; AFP, serum alpha-fetoprotein; NS, not significant between any groups or combinations thereof.

firmed that overexpression of gankyrin increased the IGFBP-5 mRNA levels 5.2-fold and 1.7-fold (mean, n = 3 each) in U-2 OS and Huh-7 cells, respectively, and western blot analysis demonstrated that the protein levels were increased as well (Fig. 4A). Conversely, when gankyrin expression was suppressed by siRNA, IGFBP-5 expression was down-regulated (Fig. 4B). In 2 of 3 HCC tissues overexpressing gankyrin, the levels of IGFBP-5 protein were higher compared with those in noncancerous tissues (Fig. 1C). To identify a role that IGFBP-5 might play in HCC cells, we next suppressed IGFBP-5 expression by siRNA. No apoptosis was induced, but viable cell numbers were decreased in Huh-7 as well as U-2 OS cells (Fig. 4C,D, and data not shown), suggesting a growth-promoting effect of IGFBP-5.

The expression of IGFBP-5 was further examined immunohistochemically in 43 HCC and 32 noncancerous liver tissues (Fig. 5, Table 3). In 42% of HCCs, IGFBP-5 was positively stained in the cytoplasm of HCC cells (Fig. 5A). IGFBP-5 was also detected, although at lower levels, in the cytoplasm of hepatocytes in 28% of the noncancerous tissues (Fig. 5B-D), but not in bile duct cells, blood endothelial cells, or other nonparenchymal cells.

Specific cytoplasmic staining for IGFBP-5 in HCC cells was associated with low TNM stage (stage I or II; $P = 0.013$), no portal venous invasion ($P = 0.006$), low serum alpha-fetoprotein value ($P = 0.031$), and small tumor size ($P = 0.009$). No association with capsular invasion or intrahepatic metastasis was observed. There was a significant association between positivities for IGFBP-5 and

**Table 3. Gankyrin Expression and Molecular Histological Markers**

| | Gankyrin Expression in HCC | | |
|---|---|---|---|
| | Negative | Positive | *P* value |
| Gankyrin expression in non-HCC | | | |
| Negative (n = 15) | 8 | 7 | 0.021 |
| Positive (n = 17) | 2 | 15 | |
| p53 expression in HCC | | | |
| Negative (n = 30) | 11 | 19 | 1.000 |
| Positive (n = 13) | 5 | 8 | |
| MDM2 expression in HCC | | | |
| Negative (n = 33) | 14 | 19 | 0.276 |
| Positive (n = 10) | 2 | 8 | |
| IGFBP-5 expression in HCC | | | |
| Negative (n = 25) | 13 | 12 | 0.026 |
| Positive (n = 18) | 3 | 15 | |
| IGFBP-5 expression in non-HCC | | | |
| Negative (n = 23) | 14 | 9 | 0.011 |
| Positive (n = 9) | 1 | 8 | |

Abbreviations: HCC, hepatocellular carcinoma; non-HCC, noncancerous portion of the resected liver; IGFBP-5, insulin-like growth factor-binding protein 5.

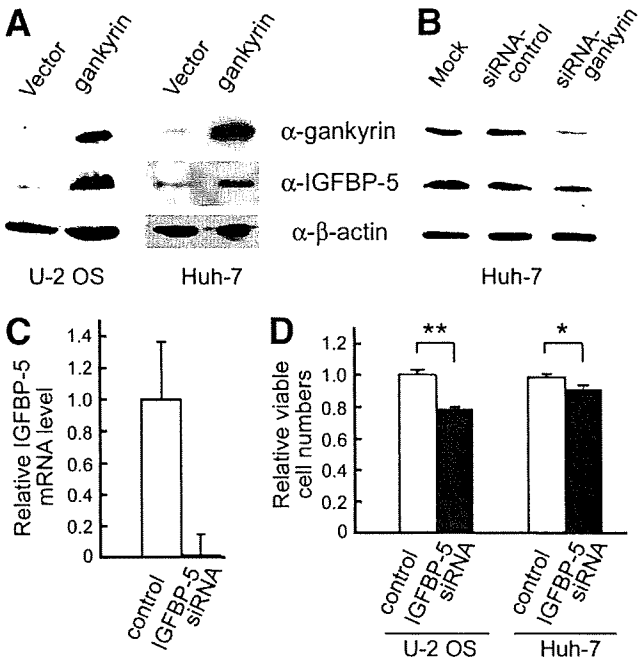


Fig. 4. Induction of IGFBP-5 by gankyrin. (A) U-2 OS cells (lanes 1 and 2) and Huh-7 cells (lanes 3 and 4) transiently transfected with plasmids expressing gankyrin or vector alone were analyzed for expression of IGFBP-5 by western blotting using the indicated antibodies. Representative results from more than 3 experiments are shown. (B) Huh-7 cells, mock transfected or transfected with siRNA for gankyrin or control RNA as indicated, were analyzed as in (A). (C) Suppression of IGFBP-5 expression by siRNA. Huh-7 cells were transfected with control RNA or IGFBP-5-specific siRNA. IGFBP-5 transcript levels were determined by real-time RT-PCR and normalized with $\beta$-actin levels. Results from 3 repeats were averaged and expressed relative to control. Error bars refer to standard deviation of the average quantitated results. (D) Effect of IGFBP-5 down-regulation on cell growth. U-2 OS and Huh-7 cells were transfected with IGFBP-5 siRNA or control RNA, and 72 hours later viable cell numbers were determined. Values are mean ± standard deviation (n = 3) and expressed relative to controls. ** and *, $P < 0.01$ and $P < 0.05$, respectively.

gankyrin (Table 3), and the levels of expression covaried both in HCCs ($\rho = 0.629$, $P < 0.001$) (Fig. 5E) and noncancerous hepatocytes ($\rho = 0.606$, $P < 0.001$) (Fig. 5F).

***Expression of Gankyrin in HCC and Patient Prognosis.*** When we examined the relationship between gankyrin expression in HCC cells and the survival of patients after surgical resection, a significant difference was observed between the patients with gankyrin-positive HCCs and those with gankyrin-negative HCCs (Fig. 6). We found no significant difference in the survival rates between the patients whose HCCs stained positively and negatively for p53, MDM2, or IGFBP-5.

## Discussion

Gankyrin is as an oncogene, mRNA of which is overexpressed in almost all human HCCs.[9,19] Although less frequent, gankyrin has been found by RNA dot blot analysis to be overexpressed in additional tumors including those of the breast, colon, rectum, stomach, small intestine, pancreas, ovary, lung, and thyroid (A. Umemura and J. Fujita, unpublished data). In the current study, we immunohistochemically examined the gankyrin protein expression in HCCs using the monoclonal anti-gankyrin antibody and found that the protein was highly expressed in the cytoplasm of 63% of HCCs. Tan et al.[20] has simi-

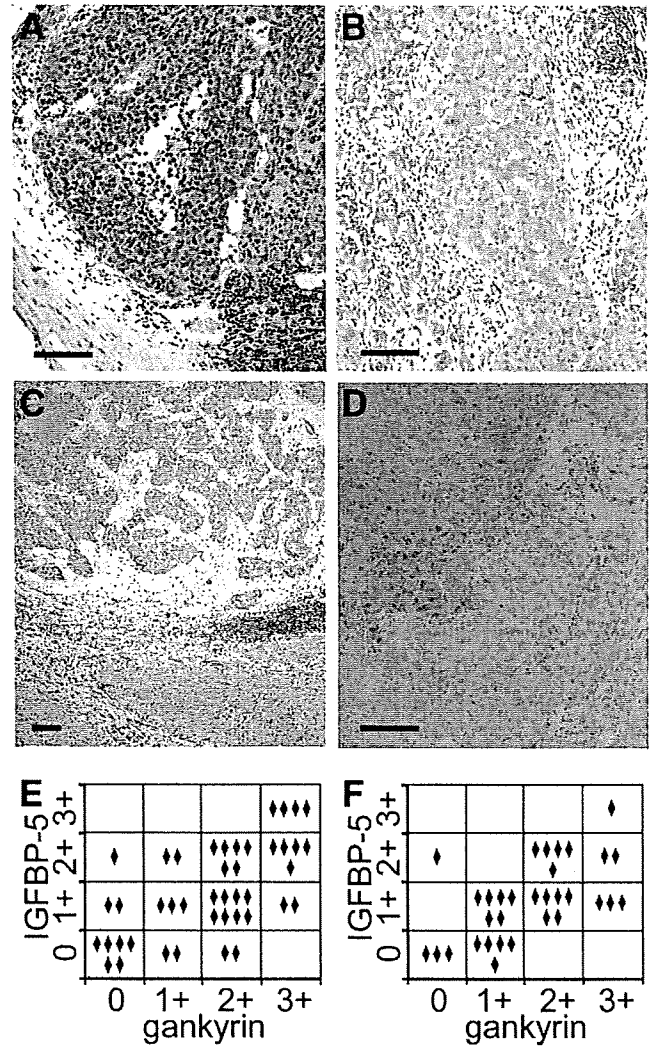


Fig. 5. Immunohistochemical detection of IGFBP-5 in hepatocellular carcinoma (HCC). HCC sections were stained with anti-IGFBP-5 antibody and counterstained with hematoxylin. Positive immunostaining appears brown. (A) Positive staining for IGFBP-5 in the cytoplasm of HCC cells, especially at the invasive boundaries. (B) Presence of IGFBP-5 in noncancerous cirrhotic hepatocytes. (C) Stronger staining for IGFBP-5 in HCC cells (upper) than the neighboring cirrhotic hepatocytes (lower). (D) Positive staining for IGFBP-5 in HCC cells (upper left), but negative in cirrhotic cells (lower right). Bar, 100 $\mu$m. (E) Correlation of expression levels of gankyrin and IGFBP-5 in HCCs. The immunostaining levels were expressed as 0 (negative), 1+ (weakly positive), 2+ (moderately positive), or 3+ (strongly positive). Each diamond represents 1 case. The Spearman's rho = 0.629, $P < 0.001$. (F) Correlation of expression levels of gankyrin and IGFBP-5 in noncancerous hepatocytes determined as in (E). The Spearman's rho = 0.606, $P < 0.001$.

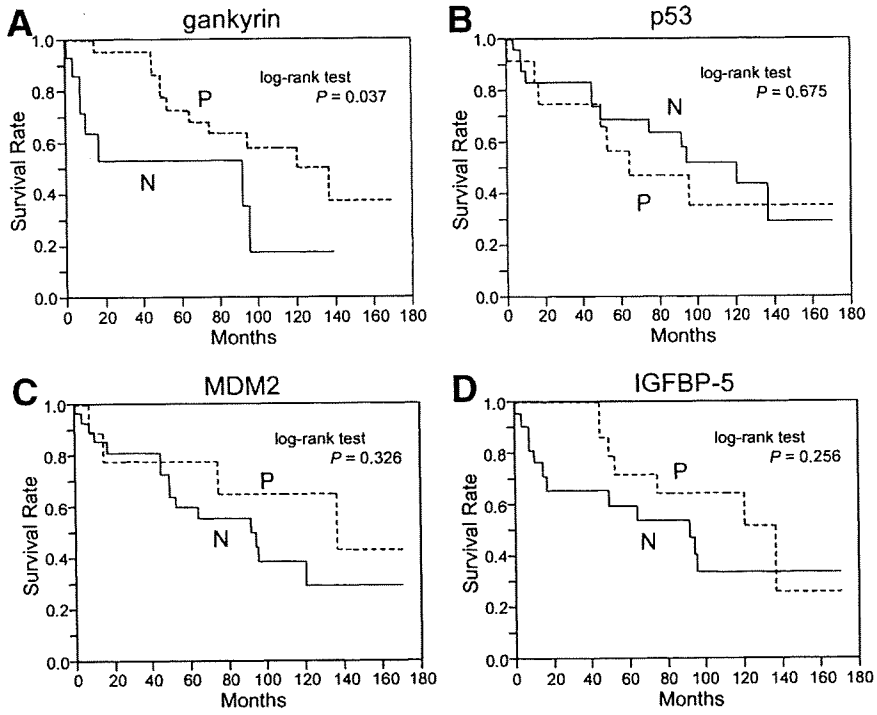


Fig. 6. Survival of patients and expression of molecular markers. The Kaplan-Meier method was used to determine the patient survival and log-rank test to compare survival between patients with HCC grouped according to (A) gankyrin positivity, (B) p53 positivity, (C) MDM2 positivity, and (D) IGFBP-5 positivity. P, positive. N, negative.

larly found overexpression of gankyrin protein in 60% of HCCs using a polyclonal antibody. The reason why the protein is not overexpressed in one-third of HCCs despite overexpression of its mRNA is unknown. The posttranscriptional, translational, and posttranslational regulations of gankyrin expression remain to be elucidated.

According to the 15th follow-up survey by the Liver Cancer Study group of Japan, the cumulative survival rates after surgical removal of HCC are 52.3% and 27.3% at 5 and 10 years, respectively, and better survival rates are associated with fewer numbers of tumors, lack of portal venous invasion, and early clinical stages.[4-6] Consistent with these observations, gankyrin positivity of HCC was associated with low TNM stage, lack of capsular invasion, portal venous invasion, and intrahepatic metastasis, and better prognosis of the patients. Patients with hyperdiploid acute lymphoblastic leukemia with more than 50 chromosomes, one of the 6 subtypes of pediatric acute lymphoblastic leukemia, have an excellent prognosis compared with other subtypes, and interestingly, overexpression of gankyrin is 1 of the diagnostic and subclassification markers for it.[21] Expression of gankyrin protein may be used as a marker for better prognosis of the patients with HCC as well.

The gankyrin oncoprotein plays a key role in regulation of cell cycle and apoptosis, at least in cultured cells, by inhibiting Rb and p53.[10] In a rodent hepatocarcinogenesis model, hypermethylation of the p16INK4A gene and p53 mutation appear at a late stage, whereas gankyrin is overexpressed from early after carcinogen treatment, preceding the loss of Rb protein and adenoma formation.[22] Clinically, p53 mutation is not so frequent in HCCs (15%-30%), especially in low-grade or low-stage HCCs.[23,24] Tan et al.[20] have immunohistochemically detected gankyrin overexpression in 82%, 63%, and 22% of Edmondson's grade I to II, III, and IV HCCs, respectively. We observed gankyrin positivity in 81% and 35% of low and high TNM stage HCCs, respectively. These results suggest that gankyrin plays an important role(s) at early stages of hepatocarcinogenesis by suppressing Rb, p53 and possibly other tumor suppressors. In advanced HCCs, by contrast, oncogenic mutations probably have accumulated in many genes including p53, and overexpression of gankyrin may not be so crucial as in early stage HCCs. This could explain the present association of gankyrin-negative HCCs with poorer prognosis and the finding that both cases of gankyrin-negative HCCs with gankyrin-positive noncancerous hepatocytes belonged to high TNM stages. This is, however, one of several possible explanations, and further work is necessary to clarify the exact reasons for the observed association.

By immunohistochemical staining, p53 has been detected in 20% to 30% of HCCs.[25, 26] Although strong immunohistochemical reactivity for p53 may not be an indicator of the presence of p53 gene mutations as initially suggested,[26] it has been associated in some studies with higher proliferative activity, lower differentiation of HCC cells, or poorer survival of patients. Endo et al.[27] immunohistochemically detected MDM2 in 28 of 107 (26%) HCCs, and the positive expression correlated with

the presence of p53 mutation and poorer prognosis, although it also correlated with smaller HCC size and the absence of vascular invasion. We immunohistochemically detected the expression of p53 and MDM2 in 30% and 23%, respectively, of HCCs, which is in accord with other studies, but no correlation was seen between expression and survival of the patients. Gankyrin accelerates degradation of Rb, p53, and MDM2 in cultured cells.[9,16] Although some correlation between expression of gankyrin and Rb has been suggested in HCC tissues,[20] we did not observe significant relationship between the gankyrin positivity and negative staining for p53 nor MDM2. The analysis of individual cells for protein expression, for example by double 2-color immunostaining, may have revealed the presence of some relationship. But most probably, our finding reflects complex interrelated mechanisms regulating the levels of these proteins and also suggests that the relevance of the effects of gankyrin on p53, MDM2, and Rb demonstrated in cultured cells to human hepatocarcinogenic process remains to be firmly established.

The 6 members of IGFBP family (IGFBP-1 through IGFBP-6) are important components of the insulin-like growth factor (IGF) axis, and regulate the activity of both IGF-I and IGF-II polypeptide growth factors.[28] IGF-I, IGF-II, and their receptors are expressed in a wide variety of cells, and the liver is the main source of circulating IGF-I. IGFBPs are also secreted by many cell types, and their expression is regulated in a cell-dependent and tissue-type–dependent manner. In the current study, we found up-regulation of IGFBP-5 mRNA and protein levels by overexpression of gankyrin in human osteosarcoma and HCC cell lines and consistently detected a significant association between the protein levels of gankyrin and IGFBP-5 in HCC specimens. In the proximal promoter region of the IGFBP-5 gene, there are several putative transcription-factor–binding sites including those for AP-2, c-Myb, C/EBP, and NF-1, and responsive elements to prostaglandin $E_2$, cyclic adenosine monophosphate, progesterone/retinoic acid, and Akt.[28] Whether the effect of gankyrin on IGFBP-5 expression is mediated by these factors is unknown.

The IGFBPs bind IGFs with high affinity, and they are able to enhance or inhibit the activity of IGFs in a cell-specific and tissue-type–specific manner.[28] In addition, IGFBPs have IGF-independent effects. There are several reports on the relationship between the IGF axis and HCC.[29-31] IGFBP-3 is the most abundant IGFBP present in noncancerous liver tissue and could serve as a negative regulator of cell proliferation in human HCCs.[32] Although the presence of IGFBP-5 in numerous tumors and cell lines has been demonstrated, its expression and significance in human HCC have not been documented. We found positive staining for IGFBP-5 in 42% of HCCs, and the positivity correlated with absence of portal venous invasion, low TNM stage, and small tumor size. Although not statistically significant, patients with IGFBP-5–positive HCCs tended to survive longer than those with IGFBP-5–negative HCCs. These findings are essentially similar to those observed for gankyrin. Regarding the effect of IGFBP-5 on cell proliferation, there are contradictory findings.[28] In breast cancer cells, many studies have reported inhibition of growth, but there are some indicating a stimulatory effect.[33] IGFBP-5 is up-regulated in involuting prostate but is also implicated in growth stimulation of prostate tumor cells.[34] We found that down-regulation of IGFBP-5 suppresses growth of Huh-7 HCC cells. Thus, these findings are consistent with a notion that high expression of IGFBP-5 and gankyrin play oncogenic roles in HCCs of early clinical stages. Clarification of the exact roles played by them will shed more light on the molecular mechanisms of human hepatocarcinogenesis and lead to development of new therapeutic and preventive strategies.

*Acknowledgment:* We thank Dr. R. John Mayer for helpful suggestions.

## References

1. Parkin DM, Bray F, Ferlay J, Pisani P. Global cancer statistics, 2002. CA Cancer J Clin 2005;55:74-108.
2. Thomas MB, Zhu AX. Hepatocellular carcinoma: the need for progress. J Clin Oncol 2005;23:2892-2899.
3. Treiber G, Wex T, Rocken C, Fostitsch P, Malfertheiner P. Impact of biomarkers on disease survival and progression in patients treated with octreotide for advanced hepatocellular carcinoma. J Cancer Res Clin Oncol 2006;132:699-708.
4. Shimada K, Sano T, Sakamoto Y, Kosuge T. A long-term follow-up and management study of hepatocellular carcinoma patients surviving for 10 years or longer after curative hepatectomy. Cancer 2005;104:1939-1947.
5. Poon RT, Fan ST, Ng IO, Lo CM, Liu CL, Wong J. Different risk factors and prognosis for early and late intrahepatic recurrence after resection of hepatocellular carcinoma. Cancer 2000;89:500-507.
6. Kiyosawa K, Umemura T, Ichijo T, Matsumoto A, Yoshizawa K, Gad A, et al. Hepatocellular carcinoma: recent trends in Japan. Gastroenterology 2004;127(5 Suppl 1):S17-S26.
7. Higashitsuji H, Higashitsuji H, Nagao T, Nonoguchi K, Fujii S, Itoh K, et al. A novel protein overexpressed in hepatoma accelerates export of NF-kappa B from the nucleus and inhibits p53-dependent apoptosis. Cancer Cell 2002;2:335-346.
8. Gotoh K, Nonoguchi K, Higashitsuji H, Kaneko Y, Sakurai T, Sumitomo Y, et al. Apg-2 has a chaperone-like activity similar to Hsp110 and is overexpressed in hepatocellular carcinomas. FEBS Lett 2004;560:19-24.
9. Higashitsuji H, Itoh K, Nagao T, Dawson S, Nonoguchi K, Kido T, et al. Reduced stability of retinoblastoma protein by gankyrin, an oncogenic ankyrin-repeat protein overexpressed in hepatomas. Nat Med 2000;6:96-99.
10. Higashitsuji H, Liu Y, Mayer RJ, Fujita J. The oncoprotein gankyrin negatively regulates both p53 and RB by enhancing proteasomal degradation. Cell Cycle 2005;4:1335-1337.
11. Hori T, Kato S, Saeki M, DeMartino GN, Slaughter CA, Takeuchi J, et al. cDNA cloning and functional analysis of p28 (Nas6p) and p40.5 (Nas7p),